CALIBRATION OF ϕ FACTORS FOR CFRP PRESTRESSED BRIDGE GIRDERS

_____

FARANAK FOROUZANNIA

Approved:

_____

Chair of the Committee
Bora Gencturk, Assistant Professor,
Civil and Environmental Engineering

_____

Co-Chair of the Committee
Mina Dawood, Assistant Professor,
Civil and Environmental Engineering

Committee Members:

_____

Abdeldjelil Belarbi, Professor,
Civil and Environmental Engineering

_____

Gino J.Lim, Associate Professor,
Industrial Engineering

_____

Suresh K. Khator, Associate Dean,
Cullen College of Engineering

_____

Roberto Ballarini, Professor,
Department Chair

CALIBRATION OF ϕ FACTORS FOR CFRP PRESTRESSED BRIDGE GIRDERS

A Thesis

Presented to

the Faculty of the Department of Civil and Environmental Engineering

University of Houston

In Partial Fulfillment

of the Requirements for the Degree

Master of Science

in Civil Engineering

by

Faranak Forouzannia

December 2014

To my parents

for their love and support

ACKNOWLEDGEMENT

I would like to express my sincere appreciation to my advisors, Professors Bora Gencturk and Mina Dawood for their valuable guidance and support throughout the course of this study at University of Houston. I am also very thankful to Professors Abdeldjelil Belarbi and Gino J. Lim for serving on my defense committee and for their comments and recommendation. I should take this opportunity to convey my thanks to my colleague Barry D.Adkins, Bora Acun, and Prakash Poudel for their help throughout this research.

I would like to express my sincere gratitude to my parents and to my sister, and brother for their constant support and love.

CALIBRATION OF ϕ FACTORS FOR CFRP PRESTRESSED BRIDGE GIRDERS

An Abstract

of a

Thesis

Presented to

the Faculty of the Department of Civil and Environmental Engineering

University of Houston

In Partial Fulfillment

of the Requirements for the Degree

Master of Science

in Civil Engineering

by

Faranak Forouzannia

December 2014

ABSTRACT

Calibration of the flexural resistance factors in the American Association of State Highway and Transportation Official's (AASHTO) Load and Resistance Factor Design (LRFD) format is performed for bridge girders prestressed with Carbon Fiber-Reinforced Polymers (CFRP). The underlying principle of the LRFD design is to achieve a uniform probability of failure (target reliability) for all possible design scenarios, which is achieved through resistance and load factors. Calibration of the resistance factors requires an extensive design space to be applicable to different design scenarios. For this purpose, 12 design cases with various span lengths, girder positions, girder spacing, roadway widths, and failure modes were considered. The load and resistance model random variables and their statistics, flexural resistance model accuracy, and the results of Monte Carlo simulation through which resistance factors were derived for different target reliabilities for interior and exterior girders failing in tension and interior girders failing in compression are presented.

TABLE OF CONTENTS

LIST OF FIGURES

LIST OF TABLES

CHAPTER 1

INTRODUCTION

1.1. Problem Statement

Sustainability is one of the most important considerations of the modern life structural design. For infrastructure, sustainability means increasing the reliability and decreasing the maintenance cost. The conventional materials of construction are prone to environmental degradation, which results in reduced structural capacity and increased maintenance.

Highway bridge structures are one of the major infrastructure components, which are subjected to the steel corrosion. In order to reduce the maintenance cost, using new materials is one option. Carbon Fiber Reinforcement Polymer (CFRP) is introduced as an alternative to reinforcing steel in the last decades. In comparison to steel, CFRP shows improved performance such as being almost two times stronger, one fifth the weight, electromagnetically resistant, and most prominently being corrosion free. These properties help reduce the amount of material used in the design, as well as the cost of maintenance.

Implementation of a new material requires an in-depth understanding of the material characteristics, the behavior of the ensuing structural member, and provisions regarding the design, serviceability, and long-term behavior. Although, there have been several studies on evaluation of CFRP performance as an alternative to prestressing steel in highway bridge girders, there is a lack of design specifications in the American Association of State Highway and Transportation Officials (AASHTO) Load and Resistance Factor Design (LRFD) format. The proposed specification should cover a

broad range of information about the design procedures, service limits, serviceability considerations, and safety issues in such a way that is efficient and applicable for the designers and contractors. The underlying principle of the LRFD design is to achieve a uniform probability of failure (target reliability) for all possible design scenarios, which is achieved through resistance and load factors. The calibration can be performed either by changing the load factors or resistant factors, or both. Since the loads are mostly independent of the materials used for reinforcing, the same load factors as proposed by latest AASHTO provision are considered in this study and calibration process is limited to the resistance factors.

1.2. Scope of Study

Calibration of resistance factors for flexural design of bridge girders prestressed with CFRP cables and bars is the main objective of this study. Monte Carlo simulation (MCS), and comparative reliability methods are used as the analysis tools. The following has been undertaken:

1) An investigation of load and resistance models and their random variables based on the available literature.
2) Development of an analytical procedure to derive the resistance factors using MCS.
3) Based on the analysis results proposing resistance factors for flexural design of bridge girders prestressed with CFRP.

1.3. Organization of the Thesis

This thesis consists of five chapters. Chapter 2 presents a review of the experimental and analytical studies that have been conducted related to this research. A brief summary of the evolution of the LRFD, properties of CFRP prestressing systems, flexural and

shear performance of the girders prestressed with CFRP, existing design guidelines for CFRP prestressing, and reliability-based studies are provided.

Chapter 3 discusses the AASHTO LRFD design load models and also provides the procedure of evaluating the capacity of the bridge girder prestressed with CFRP as a composite section. The tension and compression controlled design of beams are also addressed in this chapter.

Chapter 4 presents the reliability analysis and the obtained results. It explains the reliability analysis concepts and methods, and also provides the detailed information regarding the calibration process. It also addresses the design space considered in this study. The MCS, and comparative reliability analysis results are also included in this chapter.

Chapter 5 presents the summary and conclusions of the study. It also includes recommendations for future research.

CHAPTER 2

LITERATURE REVIEW

Civil infrastructure made of steel reinforced concrete elements is experiencing high levels of corrosion-induced damage due to the environmental attack. This can result in significant repair and maintenance costs, and in some cases results in reconstruction. In order to reduce the cost and increase the life, fiber reinforced polymers (FRPs) have been introduced as a promising substitute to steel, given their improved properties, especially resistance to corrosion. However, widespread adoption of CFRP as prestressing reinforcements for concrete bridge girders is limited due to the lack of a reliability-based design method that is consistent with the AASHTO LRFD formulation. In this chapter, a brief history of the LRFD method, previous studies on flexural behavior of CFRP prestressed beams, CFRP prestressing design guidelines, and reliability analysis of CFRP prestressed girders are presented.

2.1. LRFD Design History

A probabilistic approach is more representative of the actual behavior of a member under the induced forces and moments; however, it is more complex and time consuming for the engineering implementation. Therefore, the code specifications that adopt LRFD use load and resistance factors to account for the uncertainties associated with the demand and resistance of a member. The LRFD method is widely accepted among researchers and practicing engineers, and it has been adopted in design specifications developed by the AASHTO, the American Concrete Institute (ACI), and the American Society of Civil Engineers (ASCE). The underlying principle of the LRFD design

approach is to achieve a uniform probability of failure (target reliability) through calibrating the load and resistance factors. The generic LRFD design equation is

$$\sum \eta_i \gamma_i Q_i \leq \phi R_i, \qquad \textbf{Eq. 2-1}$$

where R_i and Q_i denote resistance and capacity, respectively, γ_i and ϕ_i are load and resistance factors and η_i is a coefficient which address the importance, redundancy, and ductility of the member under consideration. The transition from the allowable stress design (ASD) method to LRFD has first started with ACI 318 (1956) in which a model called "ultimate strength design" was proposed. The uncertainties in the design were considered by providing load factors for different load combinations. In 1963, the concept of resistance factors was introduced in the ACI 318 code. The load and resistance factors were based on engineering judgment of the committee members rather than on a reliability-based analysis. The development of LRFD codes is discussed in detail by Ravindra and Galambos (1978) and Ellingwood et al. (1980).

The LRFD method was introduced in bridge design through the National Cooperative Highway Research Program (NCHRP) Project 12-33 (Nowak, 1992) and was subsequently adopted in the first edition of the AASHTO LRFD Bridge Design Specification (1994). Nowak (1993) proposed a new live load model for the AASHTO specifications which provides uniform bias throughout different span lengths. An extensive study was performed and published in the NCHRP Report 368 (Nowak 1999), which presents the details of the new live load model, the uncertainties associated with the loads, and the calibrated load and resistance factors. The results of this study were also implemented in the most recent AASHTO LRFD specifications.

2.2. Prestressing CFRP

CFRP consists of carbon fibers embedded in a polymeric matrix (resin) in different volume percentages. The properties of the fiber and resin and the volume fraction of the fibers used in the manufacturing of the CFRP dramatically affect the properties of the resulting material. CFRP is available in the form of bars, cables, sheets, and plates, among others. Figure 2-1 shows the use of CFRP cables for internal prestressing of concrete bridge girders.

(a) (b)

Figure 2-1 (a) Typical Prestressed Bridge Girders (www.Blackburnnews.com), (b) Prestressing CFRP Cables (Enomoto and Ushijima 2012)

As mentioned earlier, CFRP provides improved properties compared to steel including resistance to electrochemical corrosion and electromagnetic radiation, high strength, and reduced weight. The strength to weight ratio of CFRP is helpful in projects such as external strengthening of bridge girders using CFRP prestressing. In this case, fewer resources are needed and the repair can be performed with minimum disruption. In addition, the corrosion resistance of CFRP eliminates the need for protection of the external prestressing.

Although CFRP has considerable advantages, there are some disadvantages of using it as the primary reinforcing system. The basic material cost of CFRP reinforcement is 5 to 15 times greater than the cost of steel reinforcements with equal tensile strength. It

should be taken in to the consideration that while the initial cost of construction using CFRP is high, the repair and maintenance cost of structures reinforced with CFRP can be much lower than those of structures reinforced with steel. Accordingly, a cost/benefit analysis should be performed to evaluate the practicality of using this kind of material. Beside the expenses, the CFRP materials show a linear elastic behavior up to failure. This might lead to a brittle, sudden failure. Other issues are the high degree of orthotropy of the materials, and high transverse thermal expansion coefficient in comparison to concrete (Roddenberry et al., 2014). The lower modulus of elasticity of CFRP materials typically results in increased deflections and crack widths which should be considered during the design process. Figure 2-2 Material Stress Strain Curvesshows the differences between the steel and other FRP material in terms of stress strain behavior in uniaxial tension.

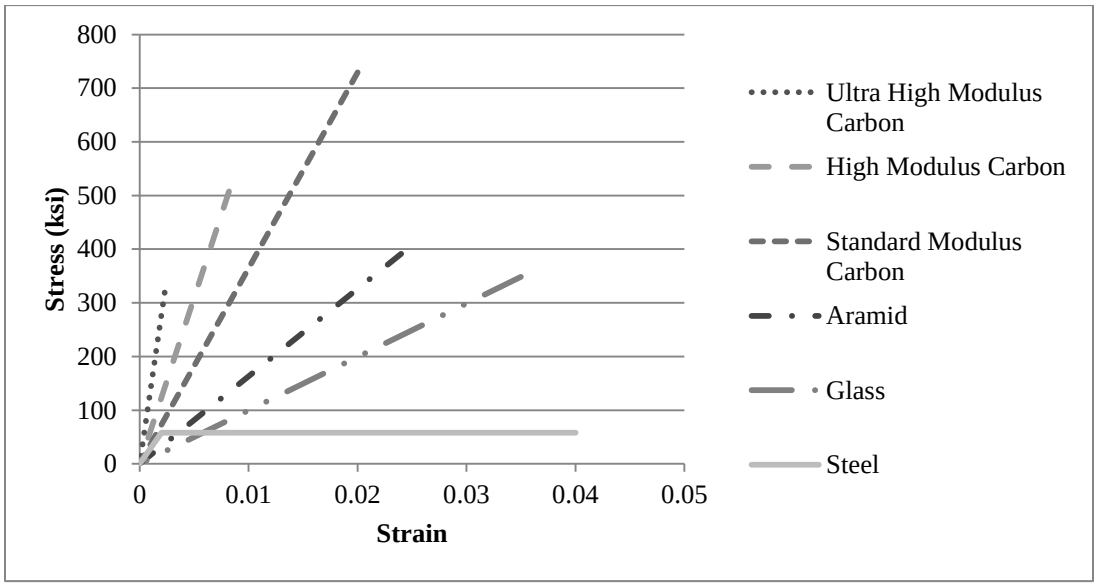

Figure 2-2 Material Stress Strain Curves

Soudki (1998) presented the material properties of FRP, and investigated the feasibility of using FRP to prestress concrete beams. The mechanical properties of CFRP

and two other types of FRP were provided and specific challenges associated with the lack of material ductility, a new design philosophy, and the effect of cyclic loading were discussed. In another study, Leung et al. (2003) investigated the practicality of using FRP in the construction industry. A brief summary of the performance of FRP materials when used as internal reinforcement in simply supported and continuous beams was provided. Additionally, previous studies using FRP for prestressing were discussed. The brittle behavior of FRP was found to be a concerning issue because of reducing ductility of the members. Based on the discussion provided in Leung et al. (2003), using of FRP for prestressing results in better utilization of the strength of the material in comparison to regular unstressed rebar. In addition, the need for a unified design code was emphasized as a barrier to the widespread adoption of FRP reinforcements for concrete structures.

2.3. CFRP Prestressed Concrete Girders

In this section, relevant research on flexural behavior of girders prestressed with bonded and unbonded CFRP is reviewed. In addition, the design methods and resistance factors proposed by the existing design guidelines are compared.

2.3.1. Flexural Behavior of Bonded CFRP Prestressed Girders

Girders prestressed with CFRP experience a sudden and brittle failure due to the brittle nature of the CFRP. Engineers are more comfortable with designing structures that provide adequate warning before failure. Concerning this issue, Abdelrahman et al. (1995) tested pretensioned T-beams. They have reported that the pretensioned system developed the full strength of CFRP tendons. Although, the brittle behavior of CFRP led to a sudden failure of the members, a considerable warning was observed before the complete failure due to formation of large, distributed cracks, and large deflections.

Due to the linear behavior of CFRP, the conventional definition of ductility is not applicable. Different definitions have been proposed by different researchers. Jo et al. (2004) provided a new definition for ductility, which is applicable for both CFRP and steel. Based on the definition provided, the ductility index is expressed in terms of total energy over elastic energy at the failure condition. An experimental study was performed to compare the ductility of beams prestressed with CFRP with that of steel prestressed beams. A total number of nine specimens with 10 inches width and 15.75 inches height were tested. The influences of tendon type, tendon bond, amount of tensile bars, and over reinforced design on the general ductility of beams were investigated. It was concluded that CFRP and steel prestressed beams show a similar behavior in terms of load-deflection, which confirms the acceptable performance of CFRP as a substitute for steel. Based on the experimental program results, the adequate deformability could be achieved by limiting the failure mode to compression control and preventing CFRP rupture.

Zou (2003) also proposed a definition of the ductility for members prestressed with CFRP. A new deformability factor was defined as the multiplication of a deflection and a strength factor. The deflection factor was defined as the ratio of the deflection at ultimate to the deflection at first cracking and strength factor was defined as the ratio of the ultimate moment to the first cracking moment. The applicability of the proposed factor was tested by an experimental program and by using data from previous experiments in the literature. It was concluded that the proposed deformability factor could capture the behavior of both CFRP and steel prestressed beams. Additionally, considerable warning was observed before the failure of the beams prestressed with CFRP.

Du et al. (2011) focused on the elastic behavior of CFRP. It was argued that the linear behavior of CFRP caused a sudden, brittle failure. Using both bonded and unbonded prestressing CFRP simultaneously was proposed as a means to enhance the deformability of CFRP prestressed concrete beams. The deformability index adopted in this study was defined as the ratio of ultimate deflection to design state deflection multiplied by the ratio of ultimate moment to the state moment. An experimental program consisting of nine specimens with 7.87×9.85 inches cross section was considered. The effect of bonded and unbonded prestressing, location of CFRP, and prestressing ratio on the flexural behavior of CFRP prestressed beams were explored. The experimental results indicated that beams prestressed with bonded CFRP had the highest flexural strength in comparison to those with externally and internally unbonded CFRP. Additionally, the load carrying capacity of the externally unbonded CFRP beams was the lowest. On the other hand, the deformability of beams prestressed with both bonded and unbonded tendons increased to some extent.

Burke et al. (2001) presented flexural design equations for beams prestressed with CFRP using strain compatibility and balance ratio concepts. For validating the flexural design model, a test program was conducted in addition to a review of previous experimental results available in the literature. The test program consisted of one T-beam with 12 inches height and 2×9.5 inches slab cross section and four rectangular beams with 7×9.5 inches dimensions. The specimens were prestressed with three different types of FRP including CFCC (Carbon fiber composite cable), Fibra 1 (aramid tendon), and Strawman (carbon fiber provided from Glasforms Inc.). It was found that the proposed design equations accurately predicted the flexural behavior of beams prestressed with

FRP. Further, the flexural resistance factor was recommended for different types of FRP by comparing the experimental capacity with the analytical capacity. The corresponding value for CFRP prestressing was recommended as 0.85. The study concluded with flexural design recommendations related to harping angle, use of multiple layers of reinforcement, and shear stirrups location through the length of beam.

In another study, Grace et al. (2006) investigated the accuracy of the strain control approach as an analysis method for flexural behavior of box beams prestressed with CFRP. In this method, the nonlinear stress-strain relationship for concrete was estimated using the equivalent rectangular stress block. The compression zone depth, strain, and curvature were also evaluated by implementing an incremental stain control approach. Six specimens were pre- and post-tensioned using bonded Diversified Composites Inc. (DCI). The first two specimens prestressed with 7 and 6 pretensioning and unbonded post tensioning DCI tendons, the second pairs pretensioned with 7 tendons, and the third pairs contain 7 and 6 pretensioned and non-prestressed unbonded post tensioning. The non-prestressed unbonded post tensioning refers to the tendons with prestressing head were anchored at both ends of specimens without any force .The study investigated the flexural performance, transfer length, deflections, and energy ratio. Experimental results confirm the practicality of the strain control approach. It was found that beams pre- and post-tensioned have greater cracking and ultimate loads compared to the beams prestressed with pre-tensioning tendons and non-prestressed unbonded post tensioning tendons. Based on the experimental data, the transfer length of 0.374 inch diameter DCI, varied between 25 to 32 times the nominal tendon diameters, which is lower than the proposed value by ACI.

Grace et al. (2012) evaluated the flexural behavior of CFRP precast decked bulb T-beams. A test program including three specimens that are 32 ft long, 14 inch deep with top and bottom flanges 18 and 12 inches wide, respectively, were considered. The specimens were partially prestressed and reinforced with different materials including Steel, CFRP Leadline, and CFCC. Experimental results confirmed that the behavior of the deck bulb T-beams prestressed with CFRP and CFCC are comparable to the beams prestressed with steel under service limits Additionally, the flexural load carrying capacity and the corresponding deflection of the CFCC prestressed beams were 107 and 94%, respectively, of those of the steel prestressed beam. In contrast, the corresponding values was determined as 88 % and 103% for CFRP beams.

The discrepancy in the thermal expansion coefficients of CFRP and concrete might lead to differential expansion of the prestressing and the concrete. Vogel and Svecova (2007) proposed an experimental study consisting of ten beams tested in flexure under thermal cyclic ranging from -40 to 40° C to measure the deterioration of bond between materials. It was found that the CFRP bars which were obtained from Hughes Brothers Inc. had excellent bond characteristics in concrete without any deterioration arising from differential expansion. Fam et al. (1997) investigated the behavior of harped prestressing CFRP on the flexural capacity of bridge I-girders. The experimental study included five specimens 30.5 ft long partially prestressed and reinforced with CFRP. One control specimen prestressed with steel was also tested. Based on the test results, specimens prestressed with CFRP and steel, exhibit similar stiffness after flexural crack pattern up to yielding of the steel. It was also found that draping of CFRP is practical and does not adversely affect the flexural capacity.

2.3.2. Flexural Behavior of Unbonded CFRP Prestressed Girders

Calibration of bridge girders prestressed with unbonded post-tensioning is out of the scope of this study. Several studies have investigated the efficiency of this method for rehabilitation of existing bridges and for new construction. This section provides a brief summary of what has been done on this subject.

The presence of unbonded prestressing requires a more complex procedure to estimate the flexural capacity. Grace et al. (2004) investigated the flexural behavior of box beams partially reinforced and prestressed using CFRP. It was reported that the combination of bonded and unbonded prestressing increased the ultimate load of the box beams by about 26% in comparison to the beam with non-prestressed unbonded post tensioning.

Aziz et al. (2005) examined the load deflection properties and ultimate load carrying capacity of the beams prestressed with bonded and post-tensioned with unbonded CFRP cables by implementing different formulations for cracked moment of inertia of concrete beam. They proposed a method, which is between two extreme cases of using bond reduction coefficient and using finite element method. In this method, the external prestressing force is assumed and two iterative loops are executed in order to calculate the strain and neutral axis depth. After satisfying the force and moment equilibrium, the total beam deflection is examined using the cracked moment of inertia. The strain, stress, and forces induced in the external unbonded cables is evaluated from the beam deflection. If the assumed value and the calculated value are equal, convergence is achieved. Using this approach, ACI (440.4R-04, 2011), Intelligent Sensing for Innovative Structures (ISIS, 2007), and Comité Euro-International duBéton - Fédération

International de la Précontrainte (CEB-FIP, 1990) deflection formulations are compared. It was concluded that ACI deflection formulation better matches with the experimental results. Additionally, using the post-tensioning force versus applied load relationship is recommended for representing the member behavior rather than the load deflection curve.

Noël and Soudki (2011) performed the experimental study in order to evaluate CFRP post-tensioned slab bridge strips flexural behavior compared to AASHTO LRFD bridge design specifications. The experimental program included 5 slabs with 11.81 inches depth and one slab with 9.85 inches depth. Five slabs reinforced with GFRP (glass fiber reinforced polymer) bars which three of them partially post tensioned using CFRP tendons. One control beam reinforced with steel tendon also tested. Based on the experimental results, the slabs prestressed with CFRP performed similar or better than the steel prestressed slabs in terms of serviceability. Additionally, the post-tensioned slabs performed satisfactorily in terms of deflection, crack width, and ultimate loads based on AASHTO LRFD design requirement.

2.3.3. Shear Behavior of CFRP Prestressed Girders

Similar to unbonded prestressing, the shear behavior of beams prestressed with CFRP and calibration of resistance factors for shear design are outside the scope of this study. This section provides a brief overview of past studies. Yonekura et al. (1994) investigated the shear behavior of beams subjected to combined torsion and bending. Fam et al. (1997) studied the shear and flexural performance of the bridge girders prestressed with CFRP tendons and reinforced with CFRP stirrups. The performances of ACI shear model (1989), and modified compression field theory (1986) in predicting the shear capacity was investigated. Sato et al. (1994) presented an analytical model for shear behavior of

beams prestressed with CFRP bars. In another study, Whitehead and Ibell (2005) proposed a shear design approach.

2.3.4. Design Guidelines

The flexural design of CFRP prestressed girders adopted by different specifications is based on cross sectional analysis, equilibrium and compatibility. A linear strain profile is assumed through the section. A nonlinear stress-strain behavior and a linear elastic stress-strain relationship are used for concrete and CFRP, respectively. In order to determine the concrete compression force, an equivalent rectangular stress block with two parameters, α and β, is used, which approximates the nonlinear stress-strain behavior of concrete. The balance ratio condition is a limit for identifying whether the member will fail in tension or in compression. The failure modes determine the stress and strain limits on the concrete and CFRP. The equilibrium has to be satisfied, using which benefits the depth of the neutral axis is found. ACI 440.4R-04 (2011) provides models for flexural and shear capacity, transfer length and flexural bond length, serviceability requirements, and information related to the material properties of FRP and anchorage systems. The ultimate concrete strain, ε_{cu}, is taken as 0.003 and rectangular stress block is used to model the concrete behavior for both tension and compression control failure modes. Both parameters α and β are taken as 0.85 for 4 ksi concrete and reduced by 0.05 per l ksi. The same procedure is implemented in this research and it will be explained in more detail in Chapter three.

ISIS (2007) also presented a guideline for design of FRP prestressed members in buildings and bridges. The FRP tendon properties, anchorage types, design procedure, serviceability limit states, etc. are considered in this specification. Different failure modes

were considered by defining a balanced condition. Unlike ACI-440 (2011), the compression control failure mode is considered to occur when the concrete ultimate strain reaches to 0.0035 before the rupture of the prestressing CFRP. Equations for evaluating α_1, β_1 in compression control failure mode are provided as a function of ultimate concrete compressive strength which is different than what proposed by ACI 440 (2011). However, in the case of tension control, the traditional rectangular stress block coefficients α_1, β_1 are not applicable. In order to handle the nonlinear concrete stress, the coefficients α and β for different ratio of existing concrete strain to the ultimate concrete strain are provided as a substitute to traditional factors.

Canadian highway bridge design code CAN/CSA-S6-06 (2006) and CSA/S806-02 (2007) also presented guidelines regarding the use of FRP prestressing in bridges and buildings, respectively. In both design guidelines, a similar procedure to that for steel is recommended for the girders prestressed with FRP with the exception that a linear stress-strain behavior is considered for the FRP. The Canadian guidelines provide the resistance factors for concrete and FRP separately. Table 2-1 shows the resistance factors adopted in the mentioned design guidelines for bonded CFRP with respect to their own specific load factors. It should be noted that these recommended values are based on engineering judgment, experience, and experimental results and not on a detailed reliability study.

Table 2-1 Resistance Factors Proposed in Existing Design Guidelines

Specification	ϕ (Tension Control)	ϕ (Compression Control)
ACI 440.4R-04 (2011)	0.85	0.65
ISIS Design Manual 5 (2007)	0.75	0.75
CSA/S806-02 (2007)	0.85	0.85
CSA-S6-06 (2006)	0.75	0.75

While the ACI 440.4R-04 (2011), adopted different resistance factors for tension control and compression control failure modes, the Canadian design specifications provide a uniform factor for different failure modes. The values provided in the Table 2-1 are not comparable between ACI 440.4R-04 (2011) and Canadian guidelines because the load factors and resistance model are different.

2.4. Reliability Analysis of Bridge Girders

It is not possible to predict the exact resistance and demand applied on a member due to the inherent randomness in the resistance and load parameters. At the same time, by adopting a reliability-based approach, the randomness can be taken into account. In this chapter, reliability studies performed on bridge girders are presented.

Calibration of AASHTO LRFD bridge design code was conducted using a probability-based approach by Nowak (1995). Nowak (1995) calibrated the load and resistance models so that the members designed based on the AASHTO code, provide a uniform reliability. A new live load model was presented and the load factors were calibrated according to the statistical parameters (dispersion and bias) of the random variables. A brief description of how the load factors were derived is provided in Chapter 3. In addition, a reliability analysis was performed in order to confirm the level of reliability of the girders and evaluate the proper resistance factors.

In a more recent study, Nowak et al. (2001) investigated the level of reliability of prestressed concrete girders designed according to different codes; namely, Eurocode (1994), Spanish Norma IAP (1998), and AAHTO LRFD (1998). Five prestressed concrete bridge girder were selected and designed according to these codes. The span lengths varied from 65.62 to 131.23ft and the girder spacing varied from 4.26 to 11.15 ft. The load and resistance parameters were treated as random variables, a reliability analysis was performed and the probability of failure was obtained. The reliability level varied considerably for the three considered codes. Eurocode (1994) was the most conservative with a reliability index between 7 and 8; while AASHTO (1998) was the least conservative with a reliability index between 4.5 and 4.9.

Okeil et al. (2002) was conducted an analytical study regarding the investigation of the flexural reliability of damaged reinforced concrete bridge girders strengthened in flexure with CFRP laminates. Three simply supported interior girders were selected with span lengths of 45, 60, and 75 ft which suffer from four different levels of steel damage. 0, 10, 20, 30% loss of cross section of reinforcing bars were assumed in order to evaluate the effect of rehabilitation on reliability level of strengthened girders. Additionally, a resistance model is proposed to predict the flexural capacity using the fiber sectional analysis concept. Other failure modes such as debonding, delamination, or shear failure were not considered in the proposed model. The applicability of the proposed resistance model was validated using the test data in the literature. Section geometry, area of steel, concrete and steel strengths, CFRP lamina strain, and model uncertainty were considered as the resistance model variables. For reducing the number of random variables, and finding the statistical parameters of resistance as a single random variable, a Monte Carlo

simulation was performed. Then an elementary first order reliability method (FORM) was implemented to find the reliability of strengthened members. The analysis demonstrated that the reliability index of strengthened cross sections is greater than that of undamaged section. Further, the reliability index of the strengthened members increased with increasing CFRP ratio. The resistance factors are calculated for the target reliabilities of 3, 3.5, 4, 4.5. Despite the higher level of reliability, a resistance factor of 0.85 was proposed for the reinforced concrete bridge girders strengthened with CFRP laminates, which is less than that in AASHTO (1998) for RC beams. The reduction in the resistance factor was due to adopting a larger target reliability index in recognition of the brittle nature of the CFRP.

Okeil et al. (2012) performed an analytical study regarding the reliability assessment of bridge girders strengthened for shear using FRP. A design model was proposed to predict the shear capacity provided by FRP strengthening sheets, while the shear capacity provided by steel stirrups, steel prestressing, and concrete were remained the same as of AASHTO LRFD specification. The reliability analysis was performed to verify the targeted reliability of the model. Three different spans lengths (45, 60, and 75 ft), two girder positions (interior and exterior), and three levels of deficiency were considered for the reliability study. Both demand and resistance parameters were considered as random variables. The girder distribution factor (GDF) statistical parameters were also presented in detail. FORM was used to evaluate the probability of failure, and the results were compared with MCS for verification. The analysis results indicated that the reliability indices are close to the target reliability varying from 3.12 to 3.5.

.CHAPTER 3

LOAD AND RESISTANCE MODELS

3.1. Introduction

An important step in calibrating the resistance factors is to identify the load and resistance models, which are used to determine the nominal demand and capacity. The selected models should be accurate and consistent with the prevailing design approaches in practice. Bridge girders are under the influence of multiple loading types such as dead load, live load, environmental load (earthquake, wind, temperature) and other loads (tire pressure, vehicle braking, and collision). All the applied loads are probabilistic and uncertain, which should be considered in the reliability-based analysis. In this study, AASHTO LRFD strength limit I is considered as the basic load combination, which includes the dead load, HL-93 live load model (which is explained below), and dynamic impact of the live load. The lateral loads due to wind and earthquake are not considered here due to the fact that these loads do not have substantial influence on the superstructure design.

The flexural capacity estimation of bridge girders prestressed with CFRP does not follow the same procedure as for steel prestressed girders due to the linear-elastic behavior of the CFRP up to failure. For this reason, as reviewed earlier, several specifications addressed the flexural behavior of composite girders prestressed with CFRP. In this research, the methodology in the ACI 440.4R-04 (2011) guideline is adopted.

3.2. Demand Model

One of the major parameters bring the uncertainty in the design, are the load models. This section provides detailed information regarding the AASHTO LRFD demand model.

3.2.1. Dead Load

Dead loads are permanent gravity loads due to structural and nonstructural elements applied on the girder for extended periods of time. Nowak (1999) performed an extensive study of existing bridge load models. The dead loads were categorized into four different groups according to their variation and type:

DFC=Weight of factory made elements (precast concrete, steel)

DCC=Weight of cast in place concrete (bridge deck)

DW=Weight of wearing surface and pavement (asphalt)

DM=Weight of miscellaneous (railing, luminaries)

3.2.1.1. Dead Load LRFD Factors

Calibration of load factors was performed by Nowak (1990) and implemented in the current AASHTO LRFD specifications. Load factors were introduced to account for the uncertainties associated with the loads in the deterministic design. The load factors are evaluated using the following equation:

$$\gamma_i = \lambda_i \times (1 + k \times COV), \qquad \textbf{Eq. 3-1}$$

where γ_i is the load factor, λ_i is the bias value (ratio of mean to nominal value), COV is the coefficient of variation (COV) and k is a constant with a recommended value equal to 2. The general interpretation of the above equation is that the load factors are directly related to the bias and standard deviation of the loads. In other words, increasing the

dispersion leads to higher load factors. Table 3-1 shows the load factors proposed by Nowak (1999).

Table 3-1 Dead Load Factors (Nowak, 1999)

Component	$\lambda_i \times (1+k \times COV)$	γ_i (Nowak, 1999)
Factory-made Elements (DFC)	$1.03 \times (1+2 \times 0.08)=1.19$	1.25
Cast-in-place Elements (DCC)	$1.05 \times (1+2 \times 0.1)=1.25$	1.25
Wearing Surface (DW)	$1 \times (1+2 \times 0.25)=1.5$	1.5

According to **Table 3-1**, statistical parameters of DCF, DCC, and DW are close to each other, therefore, a similar load factor was proposed for different types of dead load in order to simplify the design for engineers. Based on the recent AASHTO LRFD, factory made elements and cast in place members have the load factor equal to 1.25. The corresponding value for the wearing surface is proposed as 1.5.

3.2.2. Live Load

Live load is a temporary load whose magnitude and location might vary. The major live load applied on the bridge is due to the static and dynamic effect imparted by vehicles, which depend on various parameters such as the vehicles' longitudinal and transverse location on the bridge, their weight and axle spacing, multiple presences of vehicles on the bridge, girder spacing, stiffness of the slab, and the presence of diaphragms.

3.2.2.1 AASHTO LRFD Live Load Model

The AASHTO LRFD live load model was developed in the NCHRP 368 project (Nowak, 1999). The calibrated live load in the NCHRP 368 project (1999) provides a uniform bias factor for different span lengths unlike the previous AASHTO specifications. AASHTO LRFD HL-93 live load model consists of a combination of effects of the design truck (HS-20), design tandem, and uniform lane load. **Figure 3-2**

shows the design truck, tandem loads and axle's configuration, and lane load. According to AASHTO, the maximum effect of the following two combinations should be considered for design:

1) HS-20 and 0.64 k/ft uniformly distributed lane load
2) Design tandem and 0.64 k/ft uniformly distributed lane load

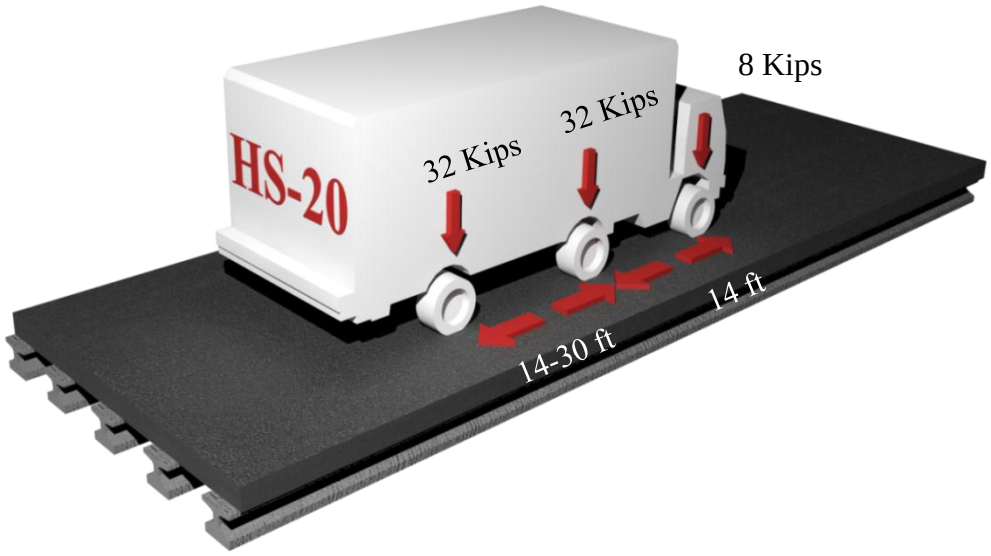

Figure 3-1 HS-20 Truck

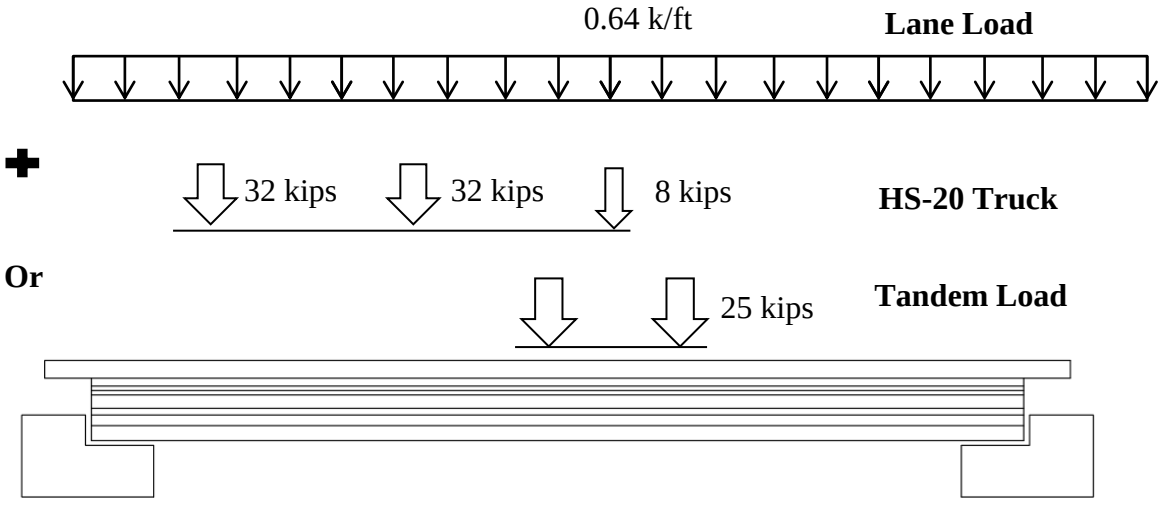

Figure 3-2 AASHTO LRFD HL-93 Live Load Model

In this research, the maximum HS-20 truck effect was obtained using the influence line method and it was compared with the results of the design tandem loading to identify the critical moment effect. The design truck load governed the design for beams with span lengths greater than 40 ft, while the tandem loading governed for shorter span girders.

3.2.2.2 Girder Distribution Factor (GDF)

GDF specifies the distribution of live load moments and shears among the different girders that are carrying load in the structure. The GDF for moment is affected by multiple parameters such as truck weight, longitudinal and transverse truck position, axle configuration, daily number of vehicles on the bridge, span length, girder position, stiffness of concrete deck, and road way width. Involvement of various parameters results in large uncertainties associated with modeling the live load. The GDF can be estimated by using different models, which are categorized into two main groups. In the first group, the GDF is calculated using a rigorous method such as finite element analysis and in the second group, it is calculated using a simplified method provided in the AASHTO Standard Specification (2002), AASHTO LRFD Specification (2005), and the Canadian Highway Bridge Design Code (2006). A recent study, NCHRP 12-62 (2007) presented a simplified method for estimating the GDF and compared the results with those from rigorous method.

Table 3-2 shows the results obtained inform the NCHRP report 592 (2007) project. It was concluded here that the AASHTO LRFD equations for moment and shear GDFs for interior and exterior girders capture the load distribution with acceptable agreement compared to the rigorous method in most cases. The excellent rating represents the cases

where the correlation coefficient between the simplified method and rigorous method is higher than 0.9. The corresponding values are between 0.9 and 0.8 for good rating and 0.8 and 0.7 for acceptable rating.

Table 3-2 Accuracy of AASHTO LRFD Girder Distribution Factor Model NCHRP 12-62 (2007)

Action	Girder locations	Lanes loaded	LRFD*
Shear	Exterior	1	Excellent
		2 or more	Acceptable
	Interior	1	Excellent
		2 or more	Good
Moment	Exterior	1	Good
		2 or more	Good
	Interior	1	Good
		2 or more	Good

*LRFD: Load and Resistance Factor Design

In this study, the simplified AASHTO LRFD method is used. Eq. 3-2 thorough Eq. 3-3 represent the AASHTO LRFD formulations (simplified methods) for moment GDF of the bridges with precast concrete I-sections as the supporting components and cast in place concrete deck.

For interior girders the moment GDF for is the maximum of the

$$\text{GDF} = 0.06 + \left(\frac{GS}{14}\right)^{0.4}\left(\frac{GS}{L}\right)^{0.3}\left(\frac{K_g}{12Lh_s^3}\right)^{0.1}, \qquad \textbf{Eq. 3-2}$$

for one lane loaded and

$$\text{GDF} = 0.075 + \left(\frac{GS}{9.5}\right)^{0.6}\left(\frac{GS}{L}\right)^{0.2}\left(\frac{K_g}{12Lh_s^3}\right)^{0.1}, \qquad \textbf{Eq. 3-3}$$

for two lane loaded, where GS is the girder spacing, L is the span length, h_s is the slab thickness, and K_g is a longitudinal stiffness parameter.

The corresponding values for the exterior girders are evaluated using lever rule for one lane loading. In this method interior girders are assumed to act as a hinge support

and the moments are taken from one support to evaluate the reaction at another support. For two or more lanes loaded, the following equation is used as

$$\mathrm{GDF}_{\mathrm{Exterior}} = \left(0.77 + \frac{d_e}{9.1}\right) \mathrm{GDF}_{\mathrm{Interior}} , \qquad \textbf{Eq. 3-4}$$

where d_e is the spacing between exterior girders and the end of the roadway.

3.2.2.3 Multiple Presence Factor (MPF)

The probability of the presence of multiple trucks on a bridge is implicitly considered in the design approach used by AASHTO LRFD. Trucks might pass side by side in different lanes or follow each other in the same lane with different headway distances. For design purposes, transverse presence of trucks is taken in to account using the multiple presence factors (MPF). AASHTO LRFD multiple presence factors are provided in Table 3-3.

Table 3-3 AAHTO LRFD Multiple Presence Factor (2010)

Number of Lane Loaded	MPF*
1	1.2
2	1
3	0.85
>3	0.65

*MPF: Multiple Presence Factor

It should be noted that the effect of the multiple presence of trucks has been reflected in developing the GDF for interior girders. Therefore, this factor should not be considered unless the lever rule method is used which is applicable to one lane loaded exterior girders. Since the girders investigated in this study are multilane loaded, this factors is not considered.

3.3. Variables in Demand Model

As it mentioned previously, the AASHTO LRFD strength limit I is implemented in this research as

$$M_{Total} = 1.25\,M_D + 1.5\,M_W + 1.75(M_{LLIM}) \times GDF, \qquad \textbf{Eq. 3-5}$$

where M_{Total} is the total demand applied on the girder, M_D is the total dead load including the cast in place concrete, and factory made elements, M_W is the wearing surface moment, and M_{LLIM} is the total live and dynamic moment per lane. In this equation, M_D, M_W, M_{LLIM}, and GDF are treated as random variables. All the variables of the demand model with their types are provided in Table 3-4.

Table 3-4 Variables in Demand Model

Variable	Notation	Type
Factory-made Elements Moment	M_D	Probabilistic
Cast-in-place Elements Moment	M_D	
Wearing Surface Moment	M_W	
Live Load per Lane Moment	M_{LLIM}	
Girder Distribution Factor Interior	GDF	
Girder Distribution Factor Exterior	GDF	
Axle Loads (Lane, HS20, Tandem)	(-)	Deterministic
Span Length	L	
Girder Spacing	GS	
Slab Thickness	t	
Longitudinal Stiffness Parameter	K_g	

3.4. Resistance Model

Due to the linear-elastic behavior of CFRP, the conventional design equations are not applicable for calculating the moment capacity of girders prestressed with CFRP. Different specifications have addressed the composite interaction between CFRP and

concrete. The methodology provided in ACI 440.4R-04 (2011) was adopted in this study. In most cases, bridge girders are designed to satisfy the service limits and they are checked for strength. Since the resistance factor is not used in the service limit combinations, and since the consideration of service limits leads to a conservative design with a higher safety margin, the service limits are not considered here.

3.4.1. Composite Behavior of Girder and Slab

Due to the sequence of loading on the composite (with the slab) and non-composite (without the slab) bridge girder section, there is a discontinuity on the induced stress and strain. The first stage of loading is the release of the prestressing force and the dead load actions coming from the girder which is followed by the application of the dead load due to the slab weight. These load effects are carried by the non-composite section (i.e., girder only). The live load and additional dead loads from the wearing surface and attachments or accessories are typically applied to the composite section.

Figure 3-3shows the stress in the section at various stages of the loading.

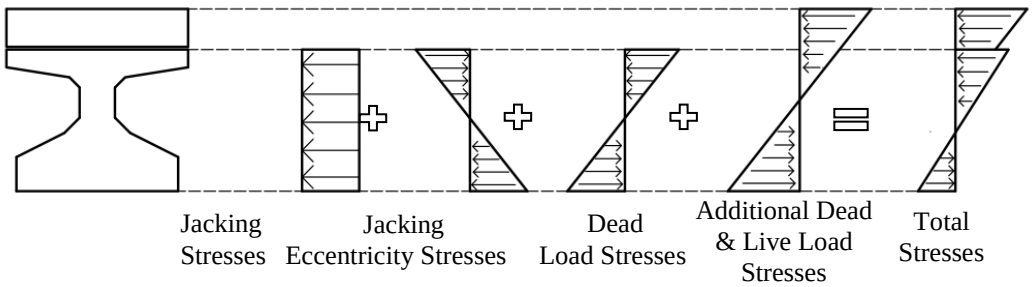

Figure 3-3 Stress Profile for the Composite Section (under Service Loading Conditions)

To evaluate the ultimate capacity of the bridge girders, the stress and strain discontinuity at the slab-to-girder interface is ignored for design purposes. Based on the ACI 440.4R-04 (2011), the ultimate behavior of a girder prestressed with FRP is

classified using the concept of balanced ratio. The balanced condition is defined where the CFRP rupture and concrete crushing happen simultaneously. For reinforcement ratios less than the balanced ratio, the failure is controlled by the CFRP rupture prior to the crushing of concrete, which is defined as a tension-controlled failure. In this case, the strain at the extreme surface of the concrete in compression is less than the ultimate strain of concrete (taken as 0.003) and leads to an approximately linear stress behavior in concrete, specially for the cases where prestressing ratio is less than half of balance ratio. However, ACI 440.4R-04 (2011) suggests using a rectangular stress block since this approach produces less than 3% error compared to elastic analysis in most cases (Burke and Dolan, 1996). The concrete compression zone is determined by iteration to satisfy the force equilibrium in the section. Figure 3-4 illustrates the stresses and strains for a tension-controlled flexural failure, where C is the concrete compressive force, f'_c concrete compressive strength, A_c is the compression zone area, T is tensile forces, f_{fi} is the FRP tensile at i layer, A_{fi} is the FRP area in layer i, ε_c is concrete strain at tip fiber, ε_{fi} is CFRP strain at layer i, ε_{pe} is the CFRP strain due to effective prestrssing force, ε_{fu} is CFRP ultimate strain and d_c and d_{Ti} are the concrete and FRP tendon moment arms, respectively.

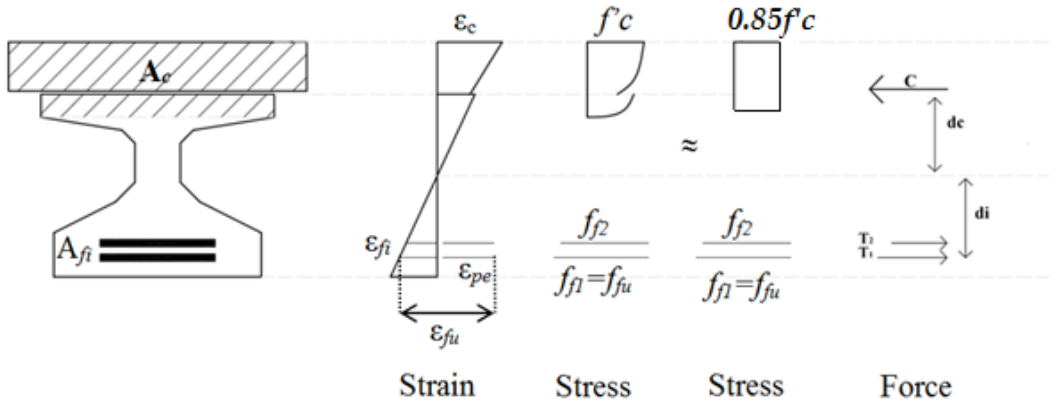

Figure 3-4 Stresses and Strains at Ultimate (Tension Control)

Determination of the moment capacity follows the flowchart shown in Figure 3-5.

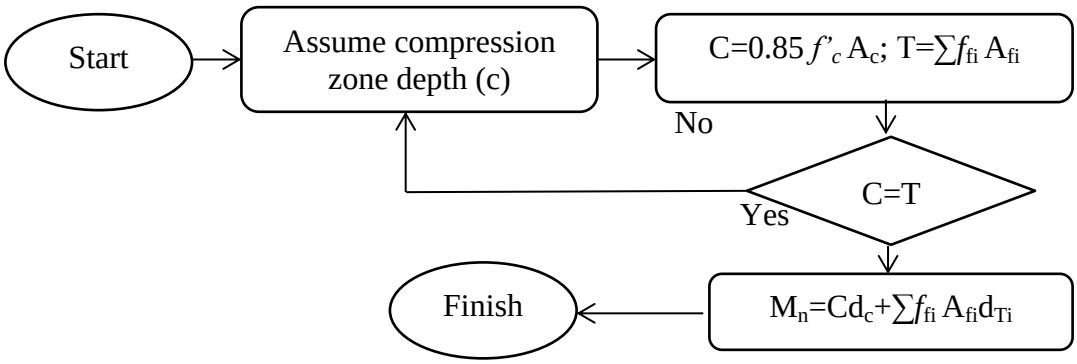

Figure 3-5 Analysis Procedure (Tension Control), the variables definition can be found in Figure 3-4

In cases where multiple layers of prestressing CFRP exist, the strain in the CFRP located at different layers is evaluated using the strain compatibility approach, considering the depth of the compression zone and the ultimate CFRP strain at the bottom-most layer as the known parameters.

In compression-controlled failures, the concrete crushes when the maximum compression strain becomes equal to 0.003 prior to the rupture of CFRP (which occurs when the tensile strain in the bottom most layer of CFRP reaches its ultimate value). Similarly, the strain in the CFRP is determined using the strain compatibility concept.

Figure 3-6 shows the distribution of stresses and strains in a compression-controlled section, where C is the concrete compressive force, f'_c concrete compressive strength, A_c is the compression zone area, T is tensile forces, ε_{fi} is FRP strain at layer i, f_{fi} is the FRP tensile at i layer, A_{fi} is the FRP area in layer i, ε_{pe} is the effective prestressing strain, ε_{pi} is the total stain at FRP located at layer i, ε_{cu} is the ultimate concrete strain, d_i is the location of FRP at layer i, and E_{Pi} is the modulus of elasticity of FRP at layer i.

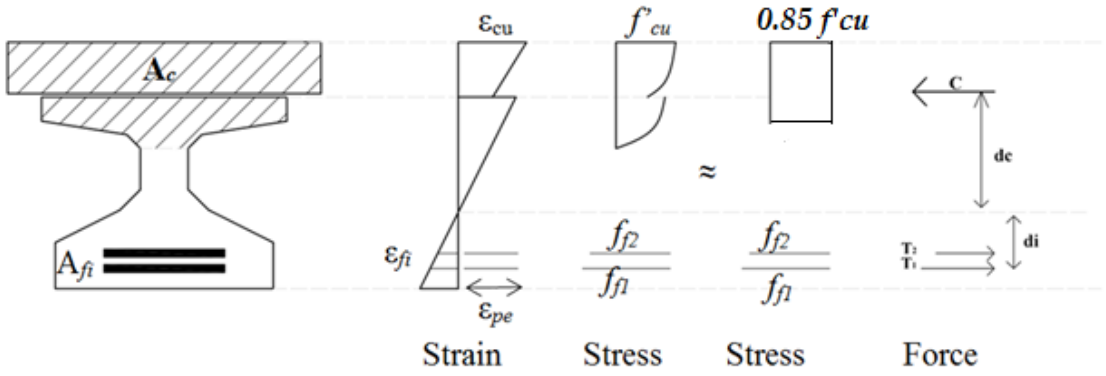

Figure 3-6 Stresses and Strains at Ultimate (Compression Control)

The procedure shown in Figure 3-7 is used to evaluate the moment capacity of girders failing by concrete crushing.

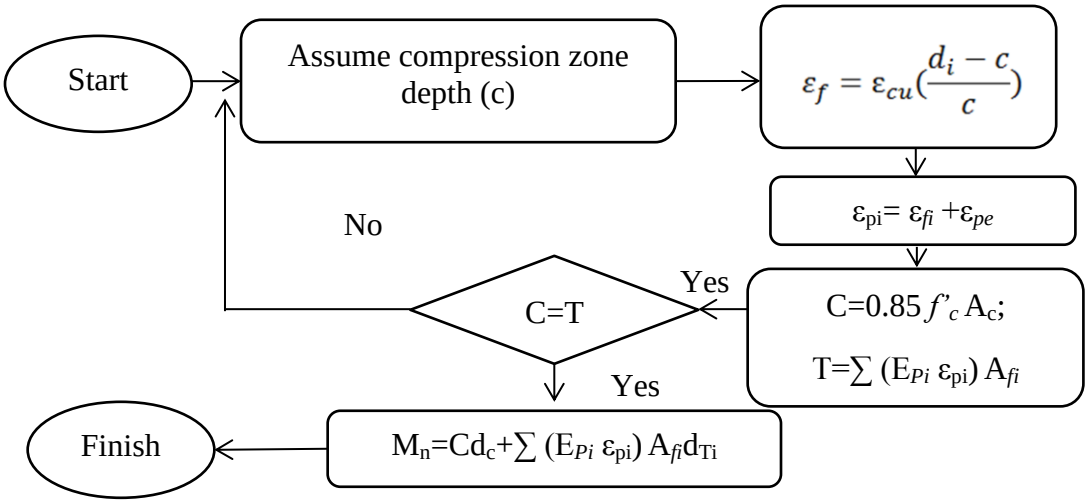

Figure 3-7 Analysis Procedure (Compression Control), the variables definition can be found in Figure 3-6

3.5. Variables in Resistance Model

Multiple variables are involved in calculation of the moment resistance as shown in Table 3-5 **Variables**. Detailed information regarding the random variables' statistical parameters is provided in Chapter 4.

Table 3-5 Variables in Resistance Model

Variable Related to	Variable	Notation	Type
Material	Concrete Compressive Strength	$f'c$	Probabilistic
	Concrete Ultimate Strain	ε_{cu}	Deterministic
	Concrete Modulus of Elasticity	E_c	Deterministic
	CFRP Tensile Strength	f_f	Probabilistic
	CFRP Effective Strain	ε_{pe}	Deterministic
	CFRP Modulus of Elasticity	E_f	Probabilistic
Geometry (Fabrication)	Slab Thickness	h_s	Probabilistic
	Girder Height	h	Probabilistic
	Tendon Arm	d_T	Probabilistic
	Concrete Arm	d_c	Deterministic
	Web Thickness	t_w	Probabilistic
	Flange Thickness	b_f	Deterministic
	Prestressing FRP area	A_f	Probabilistic
	Compression Zone Depth	c	Deterministic
Model	Professional Factor	λ	Probabilistic

CHAPTER 4

STRUCTURAL RELIABILITY ANALYSIS

4.1. Introduction

Uncertainties in evaluation of loading, material properties and geometry, and imperfect modeling of structural behavior, among others influence the probability of failure of the system. Therefore, a deterministic analysis might lead to unexpected performance. In this context, the parameters involved in the problem are categorized as deterministic or probabilistic. Structural reliability is measured in terms of a probability of failure or a reliability index. A probabilistic design approach considers this uncertainty and targets an acceptable probability of failure, which is a function of the importance of the structure and its redundancy.

Different structural reliability methods have been populated such as MCS, FORM, and Second Order Reliability Method (SORM) that differ in their complexity, implementation time, and accuracy. In this study, reliability analysis was performed using a MCS approach and a simplified comparative reliability approach.

It should be noted that a reliability analysis is time consuming and difficult to implement in comparison to a deterministic analysis; therefore, design guidelines account for the inherent uncertainty through load and resistance factors in LRFD as mentioned previously. Load and resistance factors should be calibrated in such a way that provides uniform probability of failure for different types of members having different failure modes.

4.2. Definitions

In this section basic reliability concepts including the definition of random variables, and limit state functions, are presented. A description of more general concepts is also provided in Appendix A.

4.2.1. Basic Variables

The first step in quantifying the reliability of a member is to identify the parameters contributing to the randomness of the problem. If a random variable is denoted as *xi*, a vector of $\boldsymbol{x}=\{x1, x2,\ldots,xn\}$ defines all the basic variables where *n* is the total number of random variables. The effect of variables in the evaluation of a structure's reliability depends on their statistical parameters including bias, COV, and the probability distribution function (PDF). Appendix A provides detailed definitions of the terms used in this Chapter.

4.2.2. Probability of Failure and Limit State Function

Any combination of basic random variables, which lead to a higher demand than the capacity results in the failure of a member. The basic representation of structural reliability is

$$g(Z) = R - S, \qquad \textbf{Eq. 4-1}$$

where *R* is the resistance, *S* is the demand, both of which are random variables, *Z* is another random variables defined based on Eq 4-1, and *g(Z)* is called as the limit state function. The region for which *g(Z)* is non positive is considered a failure while the region where *g(Z)* is positive is safe. The intersection region under the resistance and demand curves, as shown in Figure 4-1, illustrates the area that failure might happen. According to Figure 4-1, the type of PDF, the dispersion and the mean of the random

variables play an important role in changing the intersection region and consequently the probability of failure.

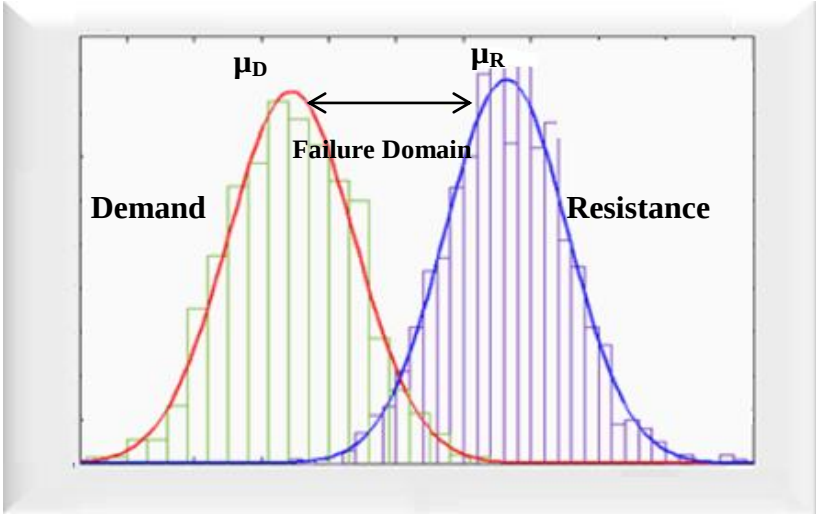

Figure 4-1 Probability of Failure Representation

The probability of failure can be evaluated by calculating the cumulative standard normal distribution of the negative of a variable called the reliability index, β, which is defined as the ratio of the mean to the standard deviation of the random variable Z as

$$P_f = \Phi(-\beta) \text{ and} \qquad \textbf{Eq. 4-2}$$

$$\beta = \frac{\mu_z}{\sigma_z}. \qquad \textbf{Eq. 4-3}$$

In general, probability of failure is characterized by the limit state function $g(Z)$ and the joint probability of distribution function $f(\boldsymbol{x})$ as

$$P_f = \int_{g(Z)\leq 0} f(x)d(x). \qquad \textbf{Eq. 4-4}$$

The joint probability distribution function represents the likelihood of a set of random variables $\boldsymbol{x}=\{x1,x2,\ldots,xn\}$ to take certain values. Probability of failure, according to Eq.

4-4 is defined as the volume under the joint PDF of the random variables where the limit state function is less than zero. The joint PDF of the random variables $\boldsymbol{x}$ can be written as

$$f(x) = f_{x_1,x_2,\dots,x_i}(x_1, x_2, \dots x_i). \quad \textbf{Eq. 4-5}$$

Integration of Eq. 4-4 becomes impractical for complex cases such as in this study, where a closed form solution to the joint PDF is not available and the number of random variable is greater than two (Der Kiureghian, 2005). Several simplified methods were proposed to perform this integration such as FORM and SORM. Another method, which is adopted herein, is the MCS, which evaluates the probability of failure directly by generating random numbers.

4.3. Monte Carlo Simulation (MCS)

Here, the probability of failure of the CFRP prestressed girders was calculated through MCS. For this purpose, *N* number of simulations were performed, in each simulation, a set of random numbers $\boldsymbol{x}$={*x1*,*x2*,…,*xn*} were generated, the demand and resistance were calculated using this information, and compared. If the set of random numbers in a given simulation makes the limit state function less than or equal to zero, this is considered a failure and the index *i* is increased by one. This process was repeated until *N* numbers of simulations were completed. The probability of failure, P_f, was then found as

$$P_f = \frac{n}{N}, \quad \textbf{Eq. 4-6}$$

where *n* is the total number of failures. The procedure for the MCS is shown in Figure 4-2.

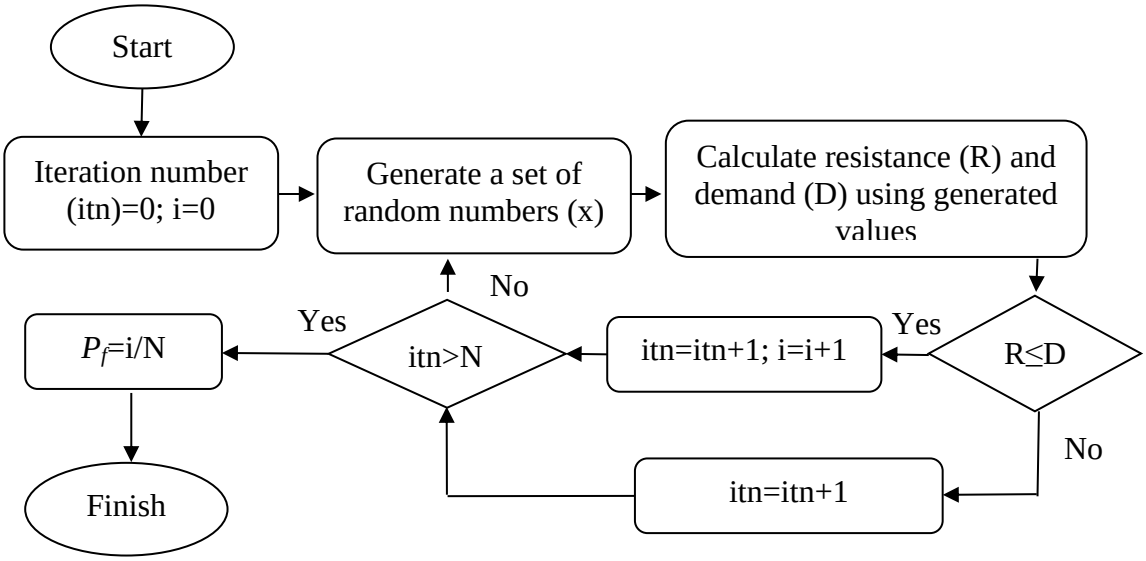

Figure 4-2 MCS Procedure

For a finite number of *N* simulations, the probability of failure is still a random number because the limit state function values evaluated from the set of random numbers might be differently distributed in the safe and failure domains. By increasing the number of simulations the dispersion of the probability of failure approaches to zero. Figure 4-3 shows the effect of *N* on the probability of failure of a 40 feet girder.

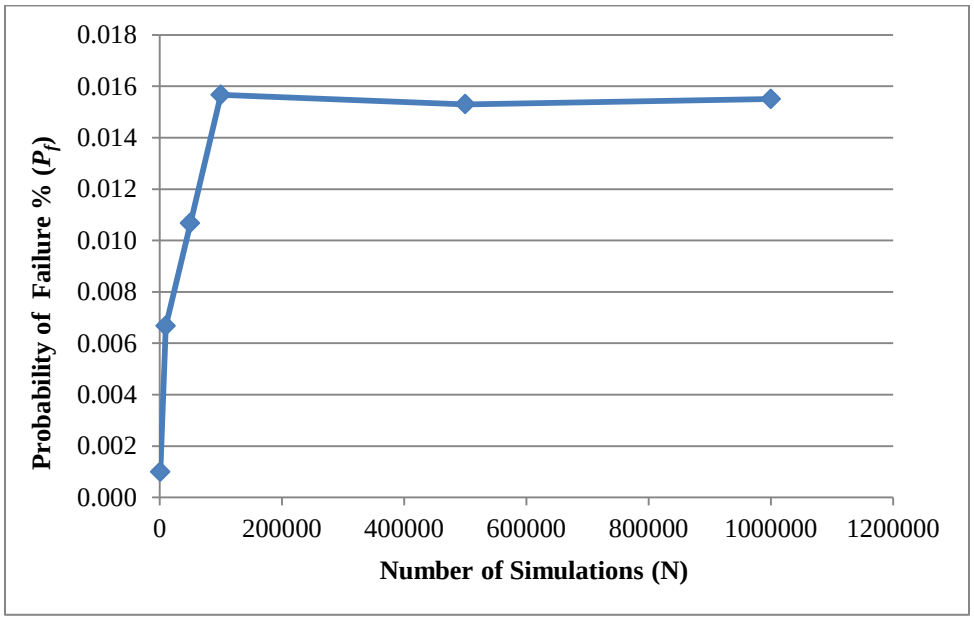

Figure 4-3 Number of Simulation Effect on Failure Probability

Although the accuracy of the results increases with increasing number of simulations, the computational demand increases as well. If the expected probability of failure is approximately known, a target number of simulations,

$$N_{Target} = \frac{1-P_f}{\delta_{Target}^2 P_f}, \quad \textbf{Eq. 4-7}$$

can be calculated as follows for a target COV, δ_{Target}.

A total of 1,000,000 simulations were performed for each case in the design space and for each resistance factor. This number of simulation corresponds to δ_{Target}=0.06 (which is deemed acceptable) for the target reliability equal to 3.5.

4.4. Statistical Properties

The statistical properties of random variables should be identified in order to perform the reliability analysis. These parameters are obtained from the databases and previous experimental results.

4.4.1. Statistical Parameters of Demand Related Random Variables

As mentioned earlier, in this study, the Strength Limit I load combination of AASHTO LRFD was used for the calibration process. This load combination includes dead load, static live load, and dynamic live load. Previous studies reported the statistical parameters of induced moments as discussed below.

4.4.1.1. Dead Load

As it was mentioned in the previous chapter, dead loads are categorized into four main groups based on their inherent variability. Nowak (1999) evaluated the statistical parameters of the moment induced by each category. The bias and standard deviation of different dead load types are provided in Table 4-1. Normal distribution function was reported for all the dead load random variables. The bias of the moment induced by the

wearing surface is based on the thickness of the pavement on the bridge which is usually 3.5 inch.

Table 4-1 Dead Load Statistical Parameters (Nowak, 1999)

Component	Bias Factor (γ_D)	COV*
Factory-made Elements (DFC)	1.03	0.08
Cast-in-place Elements (DCC)	1.05	0.1
Wearing Surface (DW)	1 (Based on 3.5 inch)	0.25
Miscellaneous Elements (DM)	1.03-1.05	0.08-0.1

*COV: Coefficient of Variation

4.4.1.2. Live and Dynamic Load

The AASHTO LRFD live load model was implemented in this study. The statistical parameters of the AASHTO live load model are well documented. Nowak (1999) performed an extensive study of this live load model. The random variables of the live and the dynamic load were reported to follow a normal distribution. The dynamic effect, multiple presences of trucks, and girder distribution factor are the required parameters for calculating live loads based on the AASHTO LRFD model. Based on Nowak (1999), girder live load moment bias factor per lane is evaluated as

$$\lambda_{LLIM} = 0.85\lambda_1\lambda_{IM}, \qquad \textbf{Eq. 4-8}$$

where λ_{LLIM} is the bias factor for live load and dynamic load moment per lane, λ_1 is the bias factor for maximum 75 year moment for a single lane, which is a function of the span length as shown in Table 4-2, and λ_{IM} is the bias factor for the dynamic load effect. While the bias factor in Nowak (1999) for λ_{IM} is 1.1, the nominal value proposed in AASHTO LRFD is 1.33, for reliability analysis, here the dynamic effect bias factor is taken as 1.1. The dynamic load effect is applied to the truck effect of the live load for evaluating the nominal moment. The coefficient 0.85 is to account for the effect of

multiple trucks passing side by side. In the case of multiple design lanes, Nowak (1999) proposed a model for two design lanes as follows

a) One lane fully loaded and the other lane unloaded.

b) Both lanes loaded. Three degrees of correlation between the lane loads are considered: no correlation ($\rho = 0$), partial correlation ($\rho = 0.5$) and full correlation ($\rho = 1$). Where ρ is the correlation coefficient.

Nowak (1999) assumed that for every 15^{th} truck on the bridge, there is another truck simultaneously on the bridge. For each simultaneous occurrence, it was assumed that every 10^{th} time, the trucks are partially correlated and every 30^{th} time, they are fully correlated (with regards to weight), which means that the probability of having two side by side fully correlated truck is equal to 1/450 (multiplication of 1/15 with 1/30). Based on the data available from truck passing observations and simulation, it was concluded that the maximum mean moment induced by two month truck loading correspond to 85 percent of 75 years truck moment (Nowak, 1999). In this study numbers of lanes loaded are higher than one.

Table 4-2 Bias Factor for Maximum 75 Year Moment per Lane (Nowak, 1999)

Span Length	Number of Lanes	Bias Per Lane
40	2	1.35
60	2	1.32
80	3	1.32
100	3	1.31
120	2	1.29

The COV's of the live load and dynamic effect were also provided in NCHRP Report 368 (Nowak, 1999). It was reported that the COV is between 19 and 20.5% per lane. For multilane bridges, this value was reported to be between 18 and 19%. The design space selected in this study includes bridges with 2 and 3 lanes; therefore, the COV of live load

and dynamic impact was selected as 18%. The difference between the moment per lane and moment per girder should be carefully considered. It should be noted that the statistical properties of the moment per girder are aimed for the reliability analysis. For this reason, GDF should be used to change the moment per lane to the moment per girder (Eq 4-5). Accordingly, the statistical properties of girder distribution factor should be taken in to account as described in the following.

4.4.1.3 Girder Distribution Factor Statistical Parameters

A coefficient, η_{GDF}, is introduced to account for the uncertainty associated with the GDF. Several studies were conducted to find the most accurate and unbiased GDF. NCHRP project 12-26 (2007) proposed shear and moment GDFs which were adopted by AASHTO LRFD. NCHRP 12-62 (2007) compared simplified methods and more rigorous methods. The COV and the bias factor for different methods were provided for different types of bridges, girder position (interior, exterior), and number of bridge lanes. The bias and COV were defined as

$$\lambda_{GDF} = \mu\left(\frac{GDF_{simplified}}{GDF_{rigorous}}\right) \text{ and} \qquad \textbf{Eq. 4-9}$$

$$COV_{\mathrm{GDF}} = \frac{\sigma\left(\frac{GDF_{simplified}}{GDF_{rigorous}}\right)}{\mu\left(\frac{GDF_{simplified}}{GDF_{rigorous}}\right)}, \qquad \textbf{Eq. 4-10}$$

where λ_{GDF} is the GDF bias, COV_{GDF} is the coefficient of variation of GDF, μ and σ are the mean value and the standard deviation of simplified method GDF to rigorous method GDF.

Of interest to this study are the moment GDFs (Eq. 3-2 and Eq. 3-3) for interior and exterior girders of multi-lane prestressed bridges.

Table 4-3 summarizes the bias and COV values of the GDF used in this study.

Table 4-3 GDF (AASHTO, 2005)/GDF (Rigorous) (NCHRP 12-62, 2007)

Girder Position	Bias	COV*
Interior	1.109	0.104
Exterior	1.208	0.221

*COV: Coefficient of Variation

Since the GDF used here followed the AASHTO LRFD formulation, the moments per girder should be divided by the ratio shown in Table 4-3. A normal distribution was reported (and used here) for this coefficient (NCHRP 12-62, 2007). In order to increase the accuracy in calculation of exterior moment GDFs, NCHRP 592 (2007) proposed a more accurate method called calibrated lever rule. With the calibrated lever rule, the bias factor and the COV are reduced from 1.208 to 1 and from 0.221 to 0.098, respectively. Since this study followed the AASHTO LRFD specification, the implementation of calibrated lever rule is not considered.

4.4.2. Resistance Statistical Parameters

Material properties, fabrication, and model errors are the three main factors contributing to the uncertainty in resistance. In this section, a detailed description of each category and their statistical properties are provided.

4.4.2.1 Materials

Several material properties including the strength and modulus of elasticity are involved in the evaluation of resistance. Environmental conditions, human errors, and instrument accuracy, among other factors affect the measured material properties. Accordingly, the properties of concrete and prestressing CFRP are considered as random variables.

The statistical properties of concrete are well-established in the literature. Nowak et al. (2003) presented the statistical properties of concrete in an effort to calibrate the ACI Building Code . A COV of 10% was adopted for concrete compressive strength and the bias factor was evaluated using

$$\lambda_{f'c} = -0.0081 f'^{3}_{c} + 0.1509\, f'^{2}_{c} - 0.9338 f'_{c} + 3.0649, \qquad \textbf{Eq. 4-11}$$

in which f'_c is in ksi.

The experimental results confirm the dependency between modulus of elasticity and compressive strength of concrete (Umoh et al., 2012). Due to this correlation, a joint probability distribution function should be used to generate random variables for modulus of elasticity and compressive strength of concrete. The degree of correlation is evaluated in terms of a correlation coefficient.

Melchers (1999) argued that for two random numbers with a correlation coefficient higher than 0.8, one can assume perfect correlation. In the case of concrete material properties, a strong linear relationship with a correlation coefficient equal to 0.807 was observed (Umoh et al., 2012). Consequently, the concrete compressive strength and the modulus of elasticity are considered as fully correlated variables in this study. For this purpose, random numbers were generated for concrete compressive strength and the modulus of elasticity, E_c, was computed using the

$$E_c = 57000\sqrt{f'_c}, \qquad \textbf{Eq. 4-12}$$

which is proposed by ACI 318-11 (2011), where f_c' is in psi.

The statistical characterization of prestressing CFRP was not performed extensively in the literature. Shield et al. (2011) reported the statistical properties of GFRP bars. Based on his report, the COV and bias factor were found to be between 0.04 to 0.12, and 1.06 to 1.22, respectively, for different bar diameters. Therefore, a conservative assumption (high dispersion and low bias) is considered here for prestressing CFRP, that is COV and bias factor were taken equal to 1.1 and 0.1, respectively. As for the modulus of elasticity of CFRP, COV equal to 0.08 and bias factor equal to 1.04 was adopted referring to the same study by Shield et al. (2011).

4.4.2.2. Geometry

Fabrication errors are considered as a source of uncertainty in structural reliability analysis. The girder and slab dimensions, prestressing CFRP eccentricity, and CFRP area are included in geometric uncertainty. The statistical parameters of girder and slab height were presented in Nowak et al. (1994). The COV and bias factor of girder and slab height were reported as 0.4/height (where height is in inch) and 1, respectively. The corresponding values of the same were suggested equal to 0.03 and 1 for the prestressing FRP area (Shield et al., 2011). In another study, Okeil et al. (2012) provided statistical information of girder web thickness and prestressing steel eccentricity. Based on the information in these studies, the statistical properties shown in Table 4-4 were implemented in this study.

Table 4-4 Statistical Properties of Random Variables Related to Geometry

Parameter	Bias	COV*	References
Slab thickness (h_s)	1	$0.4/h_s$	Nowak et al. (1994)
Girder height (h)	1	0.4/h	Nowak et al. (1994)
Tendon arm(d)	0.99	0.04	Okeil et al. (2012)
Web thickness (t_w)	1.01	0.04	Okeil et al. (2012)
Prestressing FRP area (A_f)	1	0.03	K.Shield et al. (2011)

*COV: Coefficient of Variation

4.4.2.3. Professional Factor

The resistance prediction model error should be accounted for in the structural reliability analysis. The professional factor or model error (λ) is a coefficient introduced for this purpose. For evaluating the professional factor, an extensive experimental database is required to compare the analytical solutions against. For this purpose, a database of all the available CFRP prestressed beam tests in literature was created. Twenty-nine specimens from eight studies were found to provide sufficient information that can be used to calculate the flexural capacity using the resistance model introduced in the preceding chapter (Table 4-5).

Table 4-6 Database Used to Obtain the Professional Factor

Author	Year	Analytical		Experimental		(Exp./ Analy.)
		$M_{Analy.}$	Failure Mode	M_{Exp}	Failure Mode	$M_{Exp}/M_{Anal.}$
Mutsuyoshi et al.	1990	148.22	CC*	102.23	TC**	0.690
Mutsuyoshi et al.	1990	247.44	CC	287.22	CC	1.161
Mutsuyoshi et al.	1990	180.15	CC	211.77	TC	1.175
Kakizawa	1993	70.88	TC	89.53	CC	1.263
Kakizawa	1993	70.13	CC	91.39	CC	1.303
Kakizawa	1993	45.41	TC	62.89	TC	1.385
Park And Naaman	1999	347.57	TC	533.10	TC	1.534
Abdelrahman and Rizkalla	1999	1162.63	TC	1126.88	TC	0.969
Abdelrahman and Rizkalla	1999	1083.68	TC	1039.79	TC	0.959
Abdelrahman and Rizkalla	1999	881.63	TC	958.00	TC	1.087
Abdelrahman and Rizkalla	1999	1106.40	TC	1085.45	TC	0.981
Abdelrahman and Rizkalla	1999	980.69	TC	1041.91	TC	1.062
Abdelrahman and Rizkalla	1999	656.23	TC	597.96	TC	0.911
Abdelrahman and Rizkalla	1999	634.88	TC	603.27	TC	0.950
Stoll et al.	2000	9830.40	TC	11370.12	TC	1.157
Burke & Dolan	2001	242.97	TC	308.90	TC	1.271
Burke & Dolan	2001	384.25	TC	346.97	TC	0.903
Burke & Dolan	2001	384.25	TC	346.97	TC	0.903
Burke & Dolan	2001	164.03	TC	169.06	TC	1.031
Dolan & Swanson	2002	1547.95	TC	1464.00	TC	0.946
Dolan & Swanson	2002	1547.95	TC	1392.00	TC	0.899
Mertol et al.	2006	82.10	TC	75.62	TC	0.921
Mertol et al.	2006	81.70	TC	98.69	TC	1.208
Mertol et al.	2006	81.70	TC	99.33	TC	1.216
Mertol et al.	2006	81.88	TC	96.44	TC	1.178
Mertol et al.	2006	81.85	TC	99.33	TC	1.214
Mertol et al.	2006	81.65	TC	92.92	TC	1.138
Mertol et al.	2006	81.92	TC	93.88	TC	1.146
Mertol et al.	2006	81.52	TC	88.75	TC	1.089
*CC is Compression Control; **TC is Tension Control				Average Bias		1.091

By comparing the experimental data with analytical results, the model bias, λ_γ, was evaluated as follow:

$$\lambda_\gamma = \mathrm{E}\left(\frac{\text{Experimental Flexural Capacity}}{\text{Analytical Flexural Capacity}}\right), \qquad \textbf{Eq. 4-13}$$

where *E* is the expected value operator. According to the information provided in Table 4-6, the bias and the COV were calculated as 1.091 and 0.163, respectively. Figure 4-4 compares the experimental moment with the predicted analytical moment for each of the data points in Table 4-6.

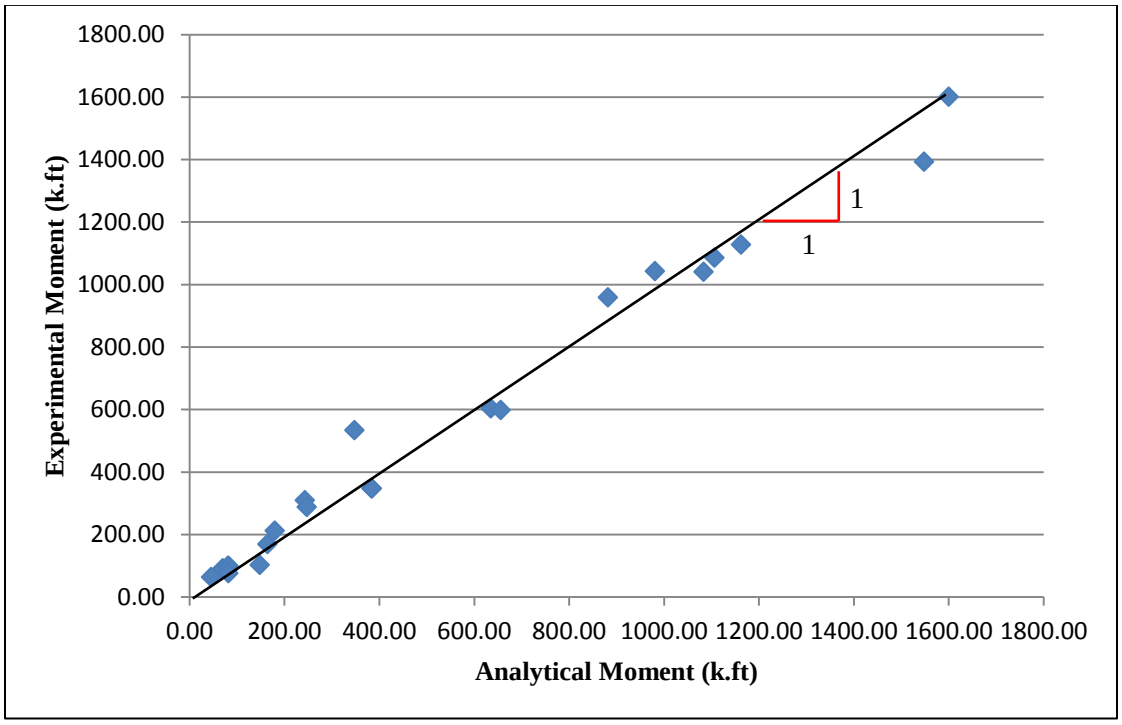

Figure 4-4 Experimental vs Analytical Moment

4.4.3. Summary of Statistical Parameters

The statistical parameters of the random variables used in this study are provided in Table 4-7. All the variables are assumed to be normally distributed.

Table 4-7 Random Variables

	Parameter	Bias	COV*	References
Resistance	Slab thickness (h_s)	1	$0.4/h_s$	Nowak et al. (1994)
	Girder height (h)	1	0.4/h	Nowak et al. (1994)
	Tendon arm(d)	0.99	0.04	Okeil et al. (2012)
	Web thickness (t_w)	1.01	0.04	Okeil et al. (2012)
	Prestressing FRP area (A_f)	1	0.03	Shield et al. (2011)
	Model Error (λ)	1.091	0.163	This Study
	Concrete Compressive Strength($f'c$)	Eq. 4-14	0.1	Nowak et al. (2003)
	CFRP Tensile Strength (f_f)	0.1	1.1	Carrol et al. (2011)
	CFRP Modulus of Elasticity (E_f)	0.08	1.04	Carrol et al. (2011)
Demand	Factory-made Elements (M_{DFC})	1.03	0.08	Nowak (1999)
	Cast-in-place Elements (M_{DCC})	1.05	0.1	
	Wearing Surface (M_{DW})	1	0.25	
	Miscellaneous Elements (M_{DM})	1.03-1.05	0.08-0.1	
	Live Load per Lane (M_{LLIM})**	1.2623	0.18	Nowak (1999)
		1.234		
		1.234		
		1.2249		
		1.2062		
	Girder Distribution Factor Interior ($\eta_{GDF,int}$)	1.109	0.104	NCHRP 592 (2007)
	Girder Distribution Factor Exterior($\eta_{GDF,Ext}$)	1.208	0.221	NCHRP 592(2007)

*COV: Coefficient of Variation ** The bias per lane varies for different span length

4.5. Design Space

The calibration of resistance factors, ϕ, for bridge girders prestressed with CFRP requires a comprehensive design space to render the results applicable to different design scenarios. However, if a larger number of parameters is included in the design space the

computational demand increases substantially. At the same time, certain variables might not have a significant influence on the capacity or demand. For this purpose, the effect of different parameters including the girder concrete compressive strength, girder depth, span length, girder position, girder spacing, roadway width, and failure mode on the moment capacity were investigated. The span length is one of the most important parameters in the design, since the maximum positive moment in simply supported girders is proportional to the square of the length. The contribution of girders in resisting the applied moment changes based on the position of girders; therefore, both internal and external girders were included in the design space. The girder spacing and roadway width were selected based on Texas Department of Transportation (TxDOT) standard specifications and drawings (TxDOT, 2014). The influence of the slab thickness and slab concrete compressive strength on the member moment capacity (for a selected girder) is investigated thorough a sensitivity analysis. Table 4-8 provides the properties of the studied girder.

Table 4-8 Properties of the Study Girder for slab thickness and slab concrete compressive strength

Length (ft)	40
Section	Tx-28
Roadway Width (ft)	24
Girder Spacing (ft)	6.67
Support Condition	Simply Supported

It is seen in Figure 4-5 that changing the slab concrete compressive strength has minimal influence on the nominal moment capacity of the girders. The same analysis was conducted to evaluate the effect of slab thickness on the nominal moment capacity as shown in Figure 4-6. A range of practical values of slab thickness was considered in the sensitivity study. It was concluded that in most cases, the concrete compressive zone is

located in the slab, therefore, changing the slab thickness did not significantly affect the moment capacity. A similar conclusion was made for the compressive strength. Therefore, 8 inch and 4 ksi were selected as practical values for slab thickness and concrete compressive strength of the slabe, respectively.

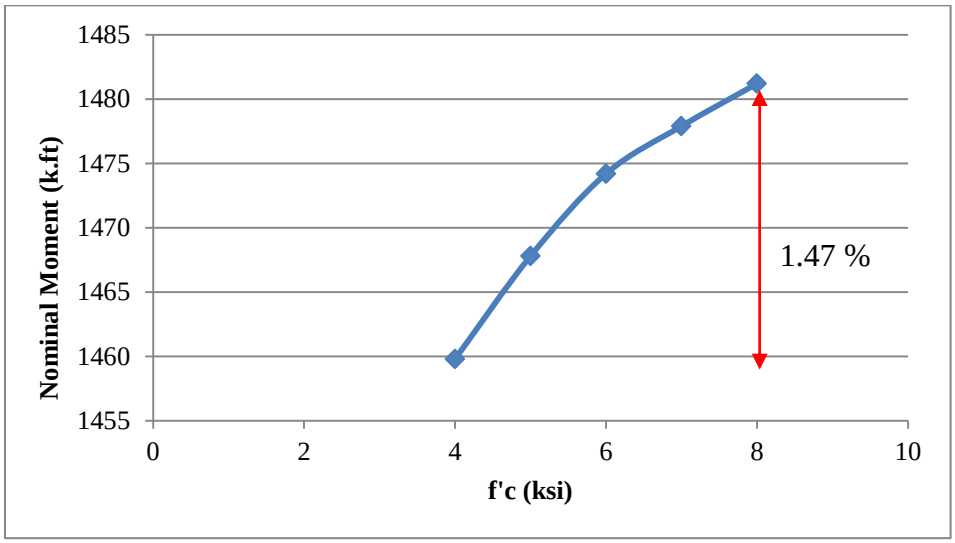

Figure 4-5 The Effect of Slab Concrete Compressive Strength on the Nominal Moment

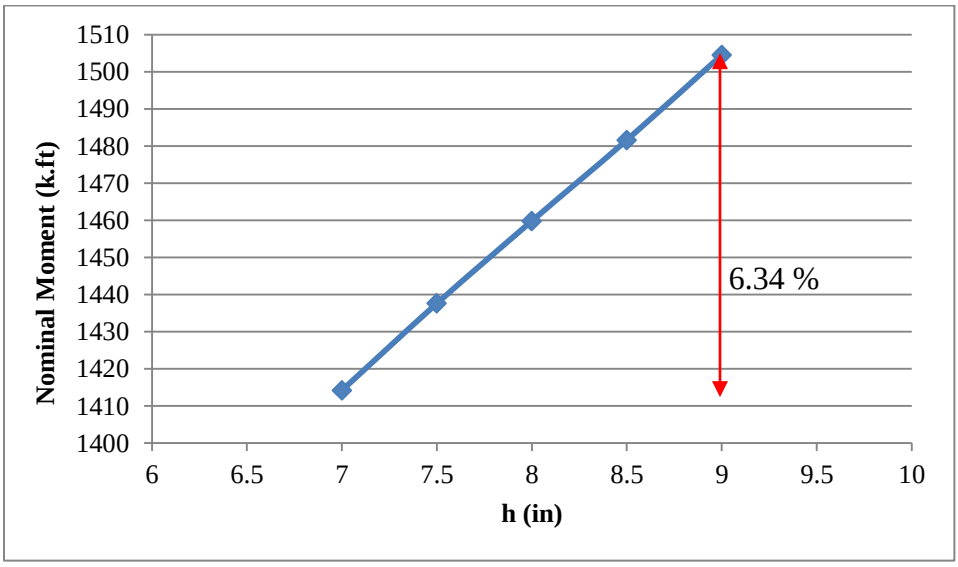

Figure 4-6 The Effect of Slab Thickness on the Nominal Moment

Different span lengths and road way widths were considered to represent different configurations of existing bridges to the extent possible. The Latin Hyper Cube Sampling

(LHCS) method was used to select the combinations of span lengths and road way widths. Table 4-9 shows the design space obtained by LHCS analysis and used here.

Table 4-9 Design Space

Span Length (ft)	Section Type	Roadway Width (ft)	Number of Girders	Girder Position	Failure Mode	Number of Cases
40	Tx 28	24	4	Internal	TC*	2
				External	TC	
60	Tx 28	32	4	Internal	TC	2
				External	TC	
80	Tx 34	40	5	Internal	TC	2
				External	TC	
100	Tx 54(TC) Tx28(CC)	38	5	Internal	TC-CC**	3
				External	TC	
120	Tx 62 (TC) Tx 28 (CC)	30	4	Internal	TC-CC	3
				External	TC	

*TC: Tension Control
**CC: Compression Control

Figure 4-7 shows the cross-sectional dimensions of the standard TxDOT sections used in this study.

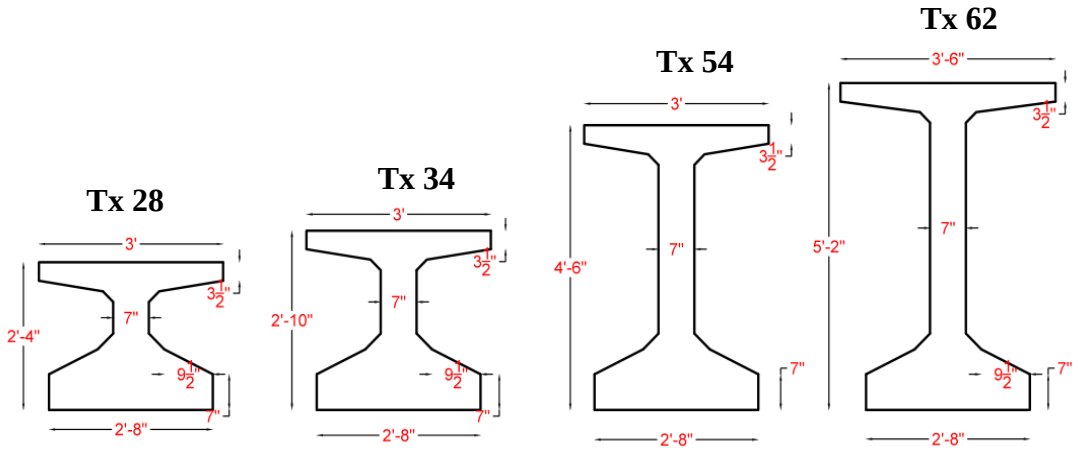

Figure 4-7 Standard TxDOT Sections

As mentioned above, the section sizes and concrete compressive strength were selected based on standard TxDOT designs (TxDOT, 2014). All bridges had an 8 inch thick slab cast on top of the girders. Girders were designed to satisfy the LRFD Strength

Limit I load combination. The concrete compressive strengths were selected as 8 and 4 ksi for the girders and the slab, respectively. Two important considerations were made in the design of the girders. First, the girders should not be overdesigned and second, the difference between the demand and resistance should remain almost constant for different cases. If the difference between the demand and capacity varies too much for different cases, the results might not be comparable. For this purpose, in finalizing the designs, different prestressing CFRP sizes were used based on the carbon fiber composite cables (CFCC) produced by Tokyo Rope (Enomoto and Ushijima, 2012).

Table 4-10 shows the properties of the CFCC used in this study.

Table 4-10 CFCC Properties (Enomoto and Ushijima, 2012)

Tendon	Diameter	Effective Area	Guaranteed Force	Guaranteed Stress (ksi)	Elastic Modulus (ksi)
1*7 7.5	0.295	0.048	17.09	354.433	22480.85
1*7 10.5	0.413	0.090	31.70	353.812	22480.85
1*7 12.5	0.492	0.118	41.36	351.144	22480.85
1*7 15.2	0.598	0.179	60.70	338.756	22480.85
1*7 17.2	0.677	0.234	78.68	335.958	22480.85
1*19 20.5	0.807	0.320	71.04	222.269	19870.17
1*19 25.5	1.004	0.472	104.99	222.293	19870.17
1*19 28.5	1.122	0.622	133.54	214.844	19870.17
1*37 35.5	1.398	0.916	189.06	206.321	18419.79
1*37 40	1.575	1.238	269.77	217.911	21030.47

4.6. Target Reliability

A target reliability index, β_T, is defined in structural reliability analysis to specify the allowable probability of failure in design. The purpose of the calibration is to find the resistance factor which meets the target the reliability. The target reliability depends on several parameters including the ductility, redundancy, failure mode, and importance of the structure. For instance, a higher reliability index is considered for a nuclear structure compared to a non-residential, non-hazardous facility. The target reliability index adopted

by AASHTO LRFD specification is 3.5. However, this value should be modified for girders prestressed with CFRP due to differences from steel prestressed girders in terms of ductility and redundancy. Allen (1992) suggested that the target reliability for a bridge system be based on the component and system behavior, inspection level, and traffic category. He added that the reliability index should be increased by 0.25 for members failing suddenly with little warning but maintaining their post failure capacity; and it should be increased by 0.5 for elements that exhibit a sudden failure with major loss of capacity. The AASHTO LRFD specifications addressed this issue by proposing the coefficient η (load modifier). This coefficient is a multiplicative combination of three parameters, η_D, η_R, and η_I which are the ductility, redundancy, and operational importance factors, respectively. η takes a value between 0.95 and 1.1 which means that the factored demand could increase or decrease depending on the characteristics of the member and the system. Increasing the ductility and redundancy, and decreasing the operational importance of the system leads to η closer to 0.95. On the other hand, brittle, systems of high importance with little redundancy require a higher load modifier. Based on the AASHTO LRFD specifications, the total load factor should be multiplied by the load modifiers to account for the diversity of the systems. Load modifiers equal to 0.95, 1, 1.05, and 1.1 corresponds to target reliabilities of 3, 3.5, 3.8, and 4, respectively.

CFRP prestressed bridge girders failing by tendon rupture suffer from a sudden failure with complete loss of capacity; however, they will show a considerable warning before failure due to the low modulus of elasticity of concrete. Based on that the two cases with different redundancy factors (both larger than 1) shown in Table 4-11 were

considered here for tension controlled failure. Table 4-11 illustrates the possible cases for the load modifier and corresponding target reliability for tension controlled failure.

Table 4-11 Target Reliability Indices for Tension Controlled Failure

Case Number	Ductility	Redundancy	Operational Importance	Load Modifier	Target Reliability
1	0.95	1.05	1	0.9975	3.5
2	0.95	1.1	1	1.045	3.8

Based on the above discussion, the target reliability equal to 3.5 and 3.8 are considered for evaluating the probability of failure for girders failing in tension.

Girders failing in compression, provide more redundancy, on the other hand, less ductility is expected from concrete crushing compared to tendon rupture. Accordingly, the redundancy and operational importance factors were considered equal to 1 and ductility factor larger than 1 was assumed as shown in Table 4-12. The target reliability indices were obtained as 3.8 and 4.0.

Table 4-12 Target Reliability Indices for Compression Controlled Failure

Case Number	Ductility	Redundancy	Operational Importance	Load Modifier	Target Reliability
1	1.05	1	1	1.05	3.8
2	1.1	1	1	1.1	4

4.7. Calibration

As presented earlier, for calibration of resistance factors, an extensive design space was considered which includes multiple girders with different live to dead load ratios. As shown in Table 4-13, the live to dead load ratio are 1.63 and 0.68 for the shortest and longest span interior girders, respectively. The corresponding values for the exterior girders are 1.84 and 0.82 for the shortest and longest span, respectively.

Table 4-13 Live to Dead Load Ratios

Span Length	Roadway Width	Section Size	Girder Position	M_{DC}* (k.ft)	M_{DW}** (k.ft)	M_{LLIM}*** (k.ft)	M_{LLIM}/ (M_{DC}+M_{DW})
40	24	TX 28	Interior	255.4	54.5	505.2	1.63
			Exterior	228.6	43.5	499.8	1.84
60	32	TX 28	Interior	689.9	170.3	1078.3	1.25
			Exterior	571.0	121.8	1067.9	1.54
80	40	TX 34	Interior	1238.1	293.0	1540.2	1.01
			Exterior	1038.8	211.6	1524.4	1.22
100	38	TX 54	Interior	2122.3	433.0	2089	0.82
			Exterior	1841.6	318.4	2067.7	0.96
120	30	TX 62	Interior	3141.8	587.1	2534.2	0.68
			Exterior	2893.7	513.7	2786.6	0.82

*M_{DC}: moment due to cast in place concrete and precast concrete
**M_{DW}: moment due to wearing surface
***M_{LLIM}: moment due to live load and dynamic impact per girder

Each girder was designed using multiple resistance factors decreasing from 1 to 0.5 in intervals of 0.05 using the appropriate load and resistance models. Figure 4-8 shows the calibration procedure for resistance factors. The calibration process includes multiple steps: definition of the design space, selecting the demand and resistance models, identifying the random variables and their statistical parameters, and conducting the reliability analysis.

As mentioned previously, MCS was used for the reliability analysis in this study. A total of 1,000,000 simulations were performed for each case in the design space and for each resistance factor. For each design scenario, the simulations start with a resistance factor equal to 1. The girder is designed such that the factored capacity becomes equal or higher than the factor loads. Number of simulations (*N*) is selected based on the accuracy required and target reliability index. The random variables involved in the demand and resistance model are identified and generated *N* times. Then, the resistance and demand are determined using the generated numbers and used to calculate the limit state function

value. This process is iterated to find the number of cases (n) where limit state function become equal or less than zero (failure condition). The simulations (itn) are continued N times. The ratio n/N gives the probability of failure (P_f). The reliability index is determined using the probability of failure. If the reliability index meets the target reliability (β_T), the resistance factor equal to 1 is an appropriate resistance factor, otherwise resistance factor is decreased by 0.05 and the process is repeated until the target reliability is reached.

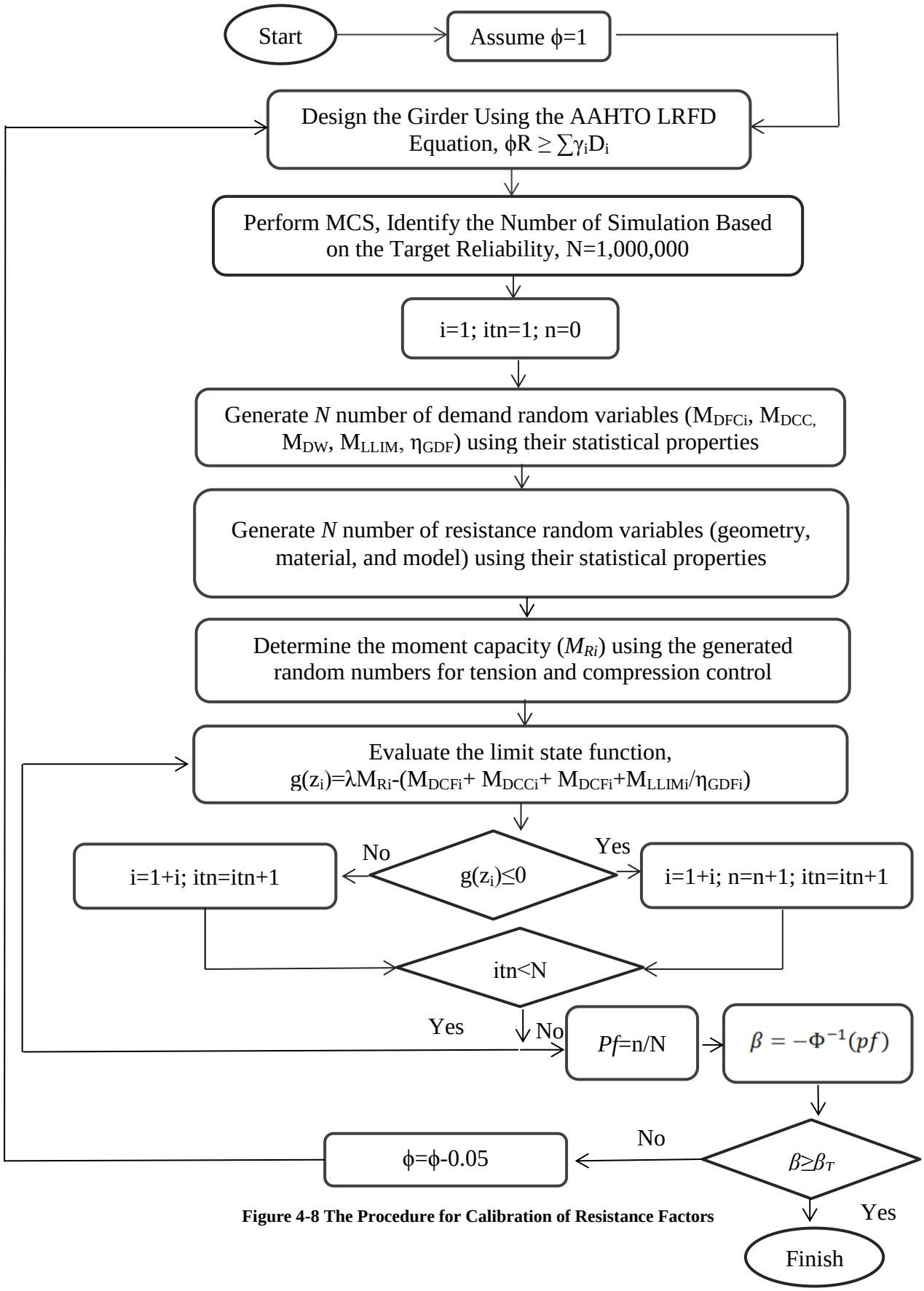

Figure 4-8 The Procedure for Calibration of Resistance Factors

Figure 4-9 and Figure 4-10 are select results showing reliability index with changing resistance factor for two interior girders with different span lengths failing in tension.

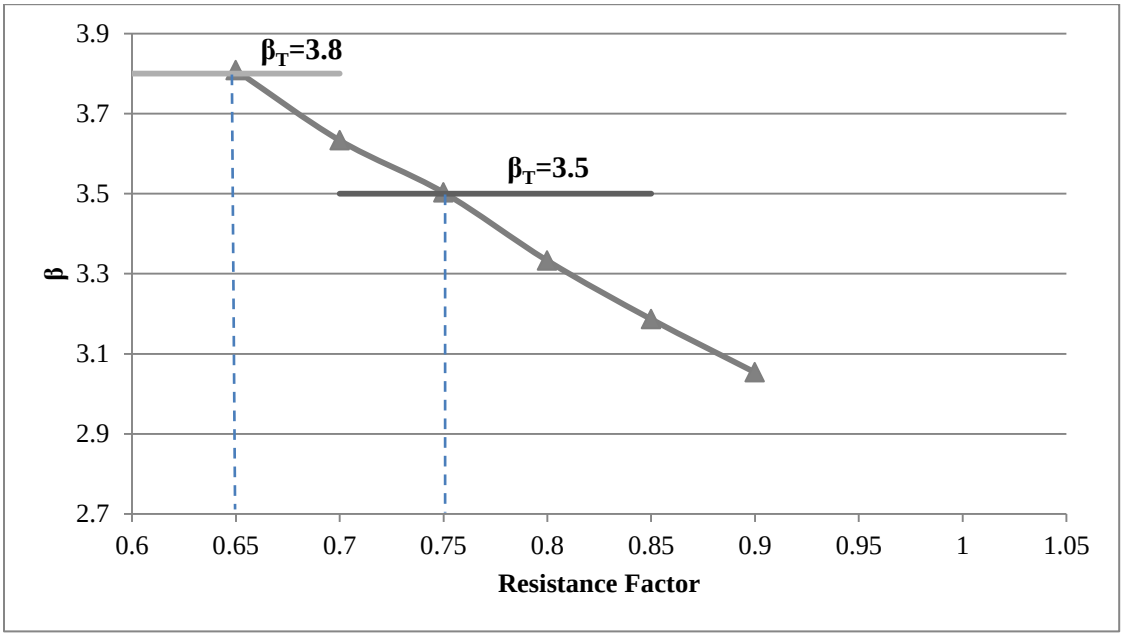

Figure 4-9 Reliability Index versus Resistance Factor (Tension Control, Int. Girder, Span Length = 80 ft)

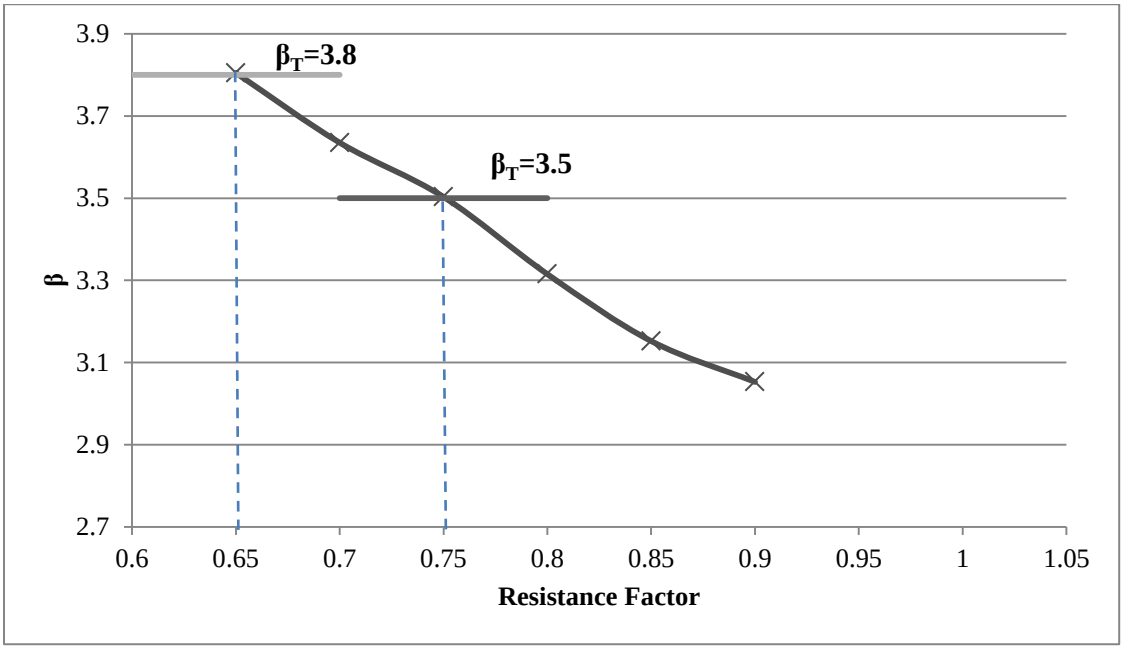

Figure 4-10 Reliability Index versus Resistance Factor (Tension Control, Int. Girder, Span Length = 100 ft)

The resistance factors corresponding to the desired target reliabilities were determined by linear interpolation from these graphs and summarized in Table 4-14. It is concluded that resistance factors equal to 0.75, 0.65, and 0.6 are appropriate for target reliabilities of 3.5, 3.8, and 4, respectively, for interior girders.

Table 4-14 Resistance Factors for Interior Girders, Tension Control

Bridge Length	Roadway Width	Section Size	Reliability Index	Resistance Factor
40	24	Tx 28	3.5	0.7607
			3.8	0.6744
			4	0.6018
60	32	Tx 28	3.5	0.7566
			3.8	0.6592
			4	0.6021
80	40	Tx 34	3.5	0.7509
			3.8	0.6523
			4	0.6024
100	38	Tx 54	3.5	0.7508
			3.8	0.6514
			4	0.6024
120	30	Tx 62	3.5	0.7500
			3.8	0.650
			4	0.6020

In calibrating the resistance factors for the exterior girders, the statistical properties of the random variables for both demand and resistance remain constant except for those of the GDF. The GDF follows a different formulation for the exterior girders and it has a higher dispersion compared to interior girders. This leads to a higher probability of failure for the exterior girders than for interior girders. Figure 4-11 and Figure 4-12 show how the reliability index changes with changing resistance factor for two exterior girders with different span lengths.

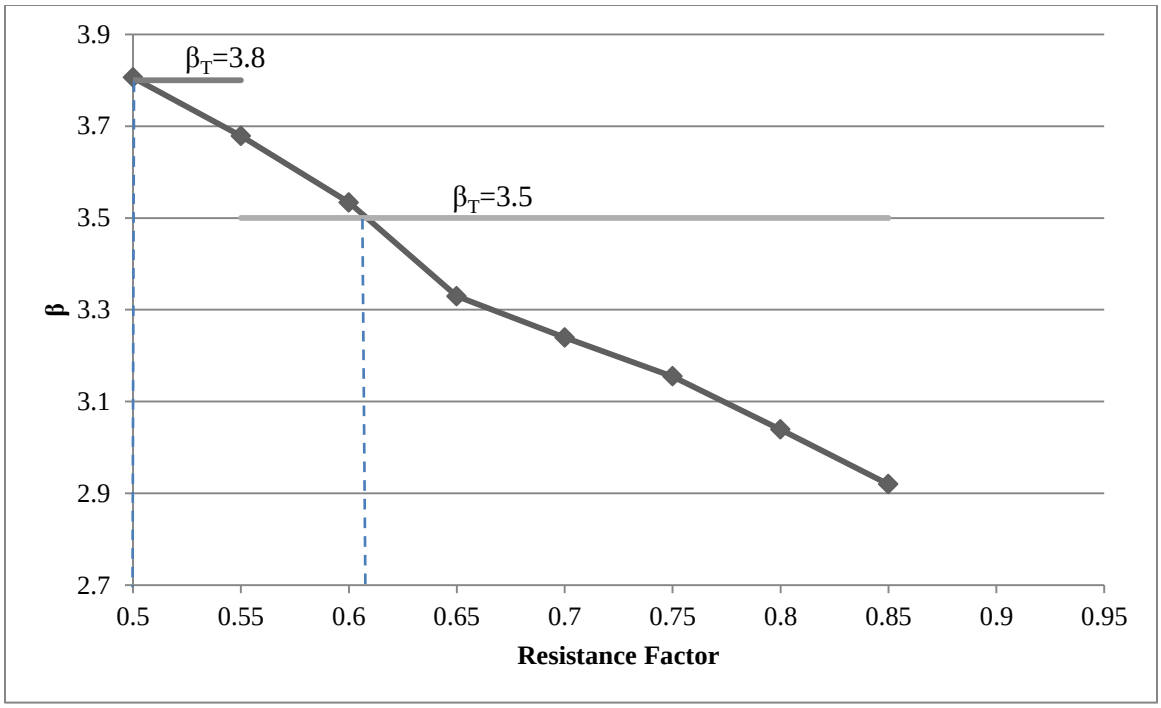

Figure 4-11 Reliability Index versus Resistance Factor (Tension Control, Ext Girder, Span Length = 40 ft)

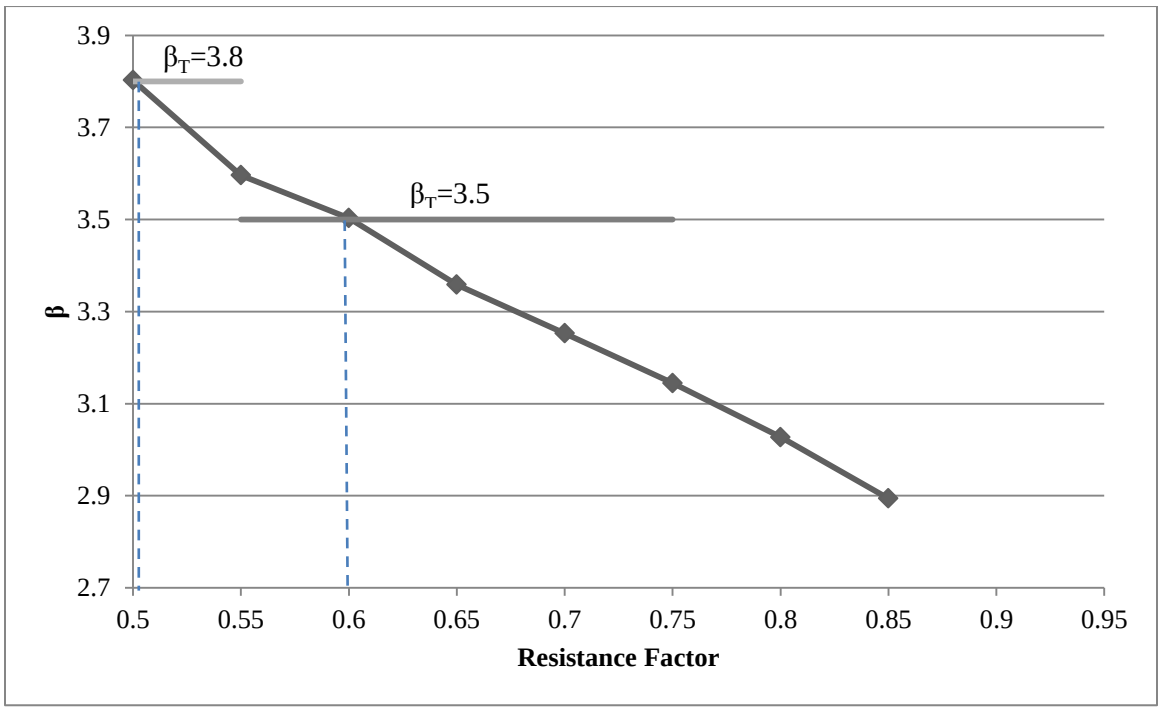

Figure 4-12 Reliability Index versus Resistance Factor (Tension Control, Ext Girder, Span Length = 60)

It is concluded that resistance factors equal to 0.6 and 0.55 are adequate for target reliabilities of 3.5 and 3.8, respectively, for exterior girders (see Table 4-15).

Table 4-15 Resistance Factors for Exterior Girders, Tension Control

Bridge Length	Roadway Width	Section Size	Beta	Resistance Factor
40	24	Tx28	3.5	0.6082
			3.8	0.5014
60	32	Tx28	3.5	0.6010
			3.8	0.5005
80	40	Tx34	3.5	0.6050
			3.8	0.5013
100	38	Tx54	3.5	0.6123
			3.8	0.5005
120	30	Tx62	3.5	0.6206
			3.8	0.5042

Comparison of Tables 4-12 and 4-13 confirms that exterior girders exhibit lower reliabilities than comparable interior girders. To reduce the uncertainty in predicting the capacity of exterior girders, which leads to a lower resistance factor for exterior girders, more accurate models for GDF should be implemented. NCHRP 592 (2007) proposed the calibrated lever rule method with higher accuracy for exterior girders. With this method, the bias factor reduces from 1.208 to 1 and the COV reduces from 0.221 to 0.098. The calibrated lever rule could be considered in future studies.

Calibrating the resistance factors for compression-controlled girders posed several challenges. First, in order to prevent overdesigning the girders, the section size (height) was decreased and larger prestressing CFRP sizes were used in some cases. For shorter span lengths, decreasing the section size was not possible because this led to section sizes that are not practical. Therefore, the design of a 40 ft long girder to fail in compression became impossible unless excessive capacity was provided. In Figure 4-13, different designs of a 40 ft long TX-28 girder is shown. Girder number 1 illustrates the

configuration required to meet the ultimate loading. In order to make the girder fail in compression, the tendon configuration should be changed to that shown for girder 3 with capacity 3.35 times the demand. Girder number 2 is an intermediate stage where the section is still tension controlled even after doubling the number of tendons. However, this leads to an underestimation of the probability of failure and overestimation of the resistance factor, which is unrealistic. Therefore, the design space for compression-controlled girders was limited to two span lengths of 100 and 120 ft. Additionally, the database used to evaluate the model uncertainty mostly includes tension-controlled girders. Therefore, the statistical properties of the model may not have been evaluated accurately for compression control. Due to the lack of information, the same model error as for tension–controlled girders was assumed in this study. Designing a girder to fail in compression was not practical for the cases where the resistance factor had to be decreased to less than 0.75. In these cases, providing more prestressing CFRP did not change the failure mode as the centroid of the prestressing CFRP shifted to the location of the neutral axis. Therefore, the probability of failure could only be calculated for the target reliability equal to 3.5.

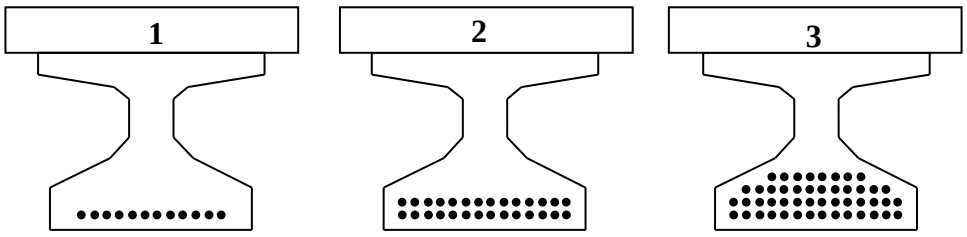

Figure 4-13 Over Designed Sections for Compression Controlled Failure

Figure 4-15 and Figure 4-15 show the reliability index as a function of the resistance factor for interior girders failing in compression. Figure 4-15 demonstrates that

the probability of failure of girders with resistance factors 1 and 0.95 are almost equal because of the additional capacity provided by compression-controlled sections as discussed above.

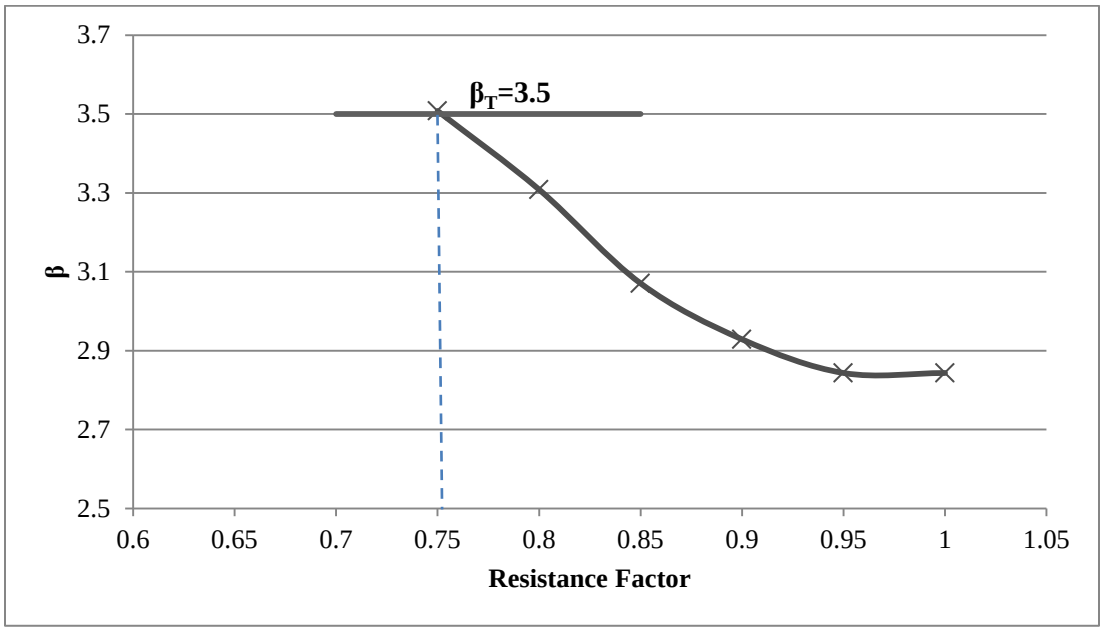

Figure 4-14 Reliability Index versus Resistance Factor (Compression Control, Int. Girder, Span Length = 100 ft)

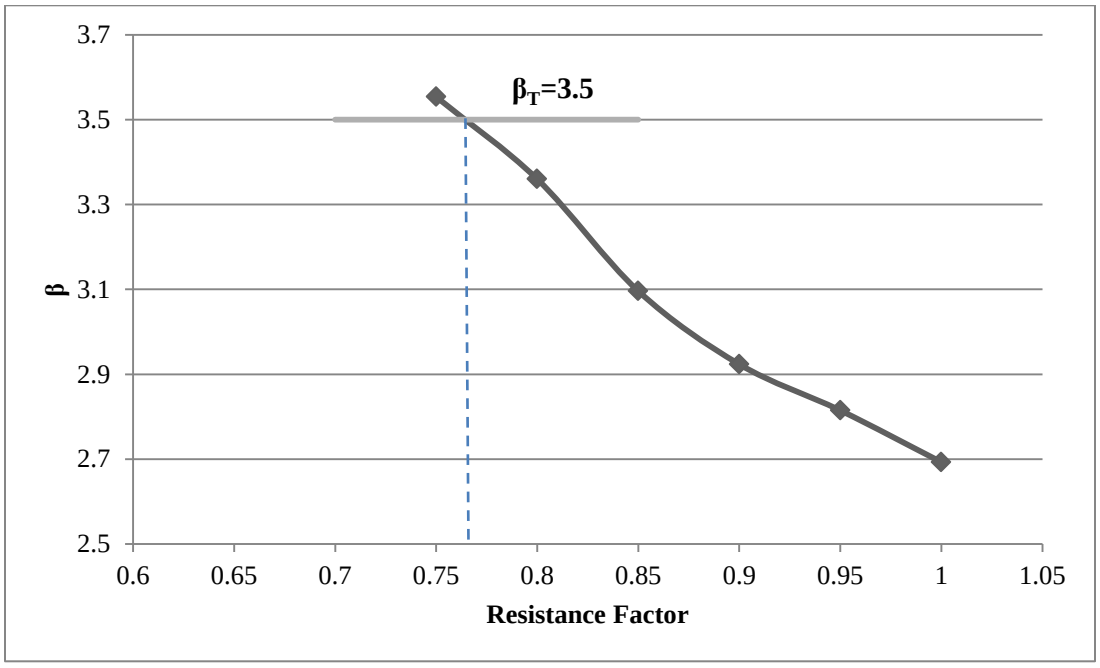

Figure 4-15 Reliability Index versus Resistance Factor (Compression Control, Interior Girder, Span Length = 120 ft)

It is concluded that a resistance factor equal to 0.75 is appropriate to achieve a reliability of 3.5 for the interior girders failing in compression (see Table 4-16). The MCS was not performed for the case of exterior girders failing in compression because the results are expected to follow a similar trend to the results for the exterior girders failing in tension.

Table 4-16 Resistance Factors for Interior Girders, Compression Control

Span Length	Roadway Width	Section Size	Beta	Resistance Factor
100	38	Tx28	3.5	0.752
120	30	Tx28		0.758

4.8. Comparative Reliability

Since the load models are the same regardless of the prestressing material, resistance model dispersion is the only parameter that changes the reliability level of a girder prestressed with CFRP from that prestressed with steel. The resistance factors for steel prestressed members are well established. By comparing the resistances of girders prestressed with steel with those of girders prestressed with CFRP, the resistance factors for CFRP prestressed girders may be derived using the concept of comparative reliability (Jawaheri Zadeh and Nanni, 2013). Comparative reliability is a method which compares a pair of elements that experience the same demand and failure type. Consequently, the resistance factor could be derived for one element by comparing the reliability levels and using a validated resistance factor of another element. A detailed description of this concept can be found in (Jawaheri Zadeh and Nanni, 2013). If the COV of the two members that are being compared is less than 0.3, the approximate formulation as

$$\frac{\ln[(\frac{\Phi_1 \lambda_2}{\Phi_2 \lambda_1})]}{\sqrt{\delta_1^2+\delta_2^2}} = \frac{\delta_2-\delta_1}{\delta_1+\delta_2}\beta_T, \qquad \textbf{Eq. 4-15}$$

can be used, where β is target reliability, and ϕ_1 and ϕ_2 are the resistance factors, λ_1 and λ_2 are the model uncertainties, , and δ_1 and δ_2 are the COVs of element 1 and 2, respectively.

If, on the other hand, the COVs of the two members being compared is larger than 0.3, the equation as

$$\frac{\ln[(\frac{\phi_1 \lambda_2}{\phi_2 \lambda_1})\sqrt{\frac{1+\delta_1^2}{1+\delta_2^2}}]}{\sqrt{\ln(1+\delta_1^2)+\ln(1+\delta_2^2)}} = \frac{\sqrt{\ln(1+\delta_2^2)}-\sqrt{\ln(1+\delta_1^2)}}{\sqrt{\ln(1+\delta_2^2)}+\sqrt{\ln(1+\delta_2^2)}}\beta_T, \quad \textbf{Eq. 4-16}$$

is implemented.

To use comparative reliability, the statistical properties of the resistance model for steel prestressed girders were obtained from the literature (Nowak, 1994). Similarly, the corresponding values for CFRP prestressed girders were obtained from the database that was explained in Section 4.4.2.3. Table 4-17 shows the values used here for comparative reliability. From the comparative reliability, the resistance factor was found to be 0.7996 for girders prestressed with CFRP, which is consistent with reliability analysis results presented above. Among all the specimens in the database, only three failed by concrete crushing. Therefore, the existing experimental database was deemed insufficient to capture the compression control resistance model properties. As a result, the resistance factor shown from this comparative analysis is only proposed for tension failure.

Table 4-17 Resistance Factor Obtained from the Comparative Reliability Method

Material	Target Reliability, β_T	Bias, λ	COV*, δ	Resistance Factor, ϕ
Steel	3.5	1.01	0.06	1
CFRP	3.5	1.091	0.163	0.7996

*COV: Coefficient of Variation

CHAPTER 5

CONCLUSIONS AND RECOMMENDATIONS FOR FUTURE RESEARCH

5.1. Summary

This study investigated the calibration of the resistance factors for CFRP prestressed bridge girders. An extensive design space which addresses various design scenarios was considered. Span length, girder position, girder spacing, and failure mode were found as the parameters that have a significant influence on the girder flexural capacity. Therefore, these were considered in a detailed reliability analysis. Monte Carlo Simulation (MCS) and a comparative reliability method were used in the calibration process. The random variables associated with load and resistance models were identified from the literature. To evaluate the model uncertainty (professional factor) a database that consists of twenty-nine specimens from eight studies were compiled. The simulation results address the resistance factors for interior girders failing in tension or compression and exterior girders failing in tension.

5.2. Conclusions

1. Based on the MCS results, for interior girders failing by CFRP rupture 0.75, 0.65, and 0.6 are proposed as resistance factors for target reliability equal to 3.5, 3.8, and 4, respectively. The resistance factor values are 0.6 and 0.5 for target reliabilities of 3.5 and 3.8 for exterior girders.
2. The comparative reliability method showed comparable results to those of the MCS. This method is straight forward, easy to use, and reduces the computational time.
3. The resistance factor for girders failing in compression follows a similar trend to those of the girders failing by CFRP rupture. The underlying reason is that similar

model, material and fabrication errors were used in the reliability analysis for both failure modes. In reality, the model dispersion may be different for different types of failure; however, there is an insufficient number of girders in literature which fail in compression to accurately assess the model uncertainty for this failure mode.

4. The probability of failure of exterior girders is higher than that of the interior girders due to higher dispersion associated with the girder distribution factor.
5. The flexural model dispersion of the girders prestressed with CFRP was determined using the experimental results from literature. A total of twenty-nine specimens from eight studies were identified. Using the compiled database, the bias and COV were found equal to 1.091 and 0.163, respectively. The model error may be improved using more data points as test results become available in the future.

5.3. Recommendations for Future Research

1. There is a lack of experimental data on CFRP prestressed girders failing by concrete crushing. The high cost of CFRP could be the main reason for not designing girders in compression control because for compression controlled design, the girders are usually overdesigned requiring more prestressing CFRP. However, in practical applications, if additional capacity is needed, it would generally be more economical to increase the overall depth of a girder while maintaining a tension-controlled failure rather than trying to impose a compression-controlled condition. Thus, the only scenario in which a compression-controlled failure is expected to dominate is for girders with high moment demands and strict depth restrictions. This subset is expected to be relatively small. Therefore, CFRP rupture is expected to be the

predominant failure mode for CFRP-prestressed concrete girders. In order to better capture the behavior of girders failing in compression, further testing is required.

2. The resistance factors for exterior girders should be investigated using more accurate GDF methods such as calibrated lever rule. The detail information regarding the application of this method can be found at NCHRP 12-62 (2007). By improving the model for exterior GDF, the reliability of exterior girders could be improved, and consequently higher resistance factors could possibly be used. The bias factor can be reduced from 1.208 to 1 and COV can be reduced from 0.221 to 0.098.It is expected that higher resistance factors will be obtained by using the more accurate GDF models having lower bias and COV values.

REFERENCES

Abdelrahman A, Rizkalla S., (1999). "Deflection Control of Concrete Beams Pretensioned by CFRP Reinforcements." J Comp Construct ;3(2):55–62.

ACI 318-11, (2011). "Building Code Requirements for Structural Concrete." American Concrete Institute.

ACI 318-56, (1956). "Building Code Requirements for Reinforced Concrete." American Concrete Institute.

ACI 440.4R-04, A., (2011). "Prestressing Concrete Structures with FRP Tendons". American Concrete Institute.

AASHTO LRFD Bridge Design Specifications, (1994). American Association of State Highway and Transportation Officials,Washington, D.C.

AASHTO LRFD Bridge Design Specifications, (2005). American Association of State Highway and Transportation Officials,Washington, D.C.

AASHTO LRFD Bridge Design Specifications, (2010). American Association of State Highway and Transportation Officials,Washington, D.C.

AASHTO Standard Specifications for Highway Bridges (2002). American Association of State Highway and Transportation Officials,Washington, D.C.

Allen, D. E., (1992). ''Canadian Highway Bridge Evaluation: Reliability Index.'' Can. J. Civ. Eng., 19(6), 593–602.

Aziz, M. A., Abdel-sayed, G., Ghrib, F., Grace, N. F., and Madugula, M. K. S., (2005). "Analysis of Concrete Beams Prestressed and Post-Tensioned with Externally Unbonded Carbon Fiber Reinforced Polymer Tendons." *Can. J. Civ. Eng*, 1151(April), 1138–1151.

BridgeTech Inc, Tennessee Technological University, and Mertz, D. R., (2007). "Simplified Live Load Distribution Factor Equations." NCHRP Report 592, Transportation Research Board, Washington, D.C.

Burke, C. R., Dolan, C. W., and Ph, D., (2001). "Flexural Design of Prestressed Concrete Beams Using FRP Tendons." *PCI Journal*.

CAN/CSA-S6-06., (2006). "Canadian Highway Bridge Design Code." Canadian Standards Association, Ontario, Canada;

CSA/S806-02, (2007). "Design and Construction of Building Components with FibreReinforced Polymers." CAN/CSA, Canadian Standards Association, Rexdale, Ontario, Canada;

Der Kiureghian, Armen., (2005). “First- and Second-Order Reliability Methods.”

Dolan, C. W., and Swanson, D., (2002). “Development of Flexural Capacity of a FRP Prestressed Beam with Vertically Distributed Tendons.” 33, 1–6.

Ellingwood, B., Galambos, T. V., MacGregor, J. G., and Cornell, C. A., (1980). “Development of a Probability Based Load Criterion for American National Standard A58.”

Enomoto, Tsuyoshi, and Ushijima, Kenichi, (2012). “ Use of CFCC Tendons and Reinforcements in Concrete Structures for Durability.”

Grace, N. F., Singh, S. B., Shinouda, M. M., and S.Mathew, S., (2004). “Flexural Response of CFRP Prestressed Concrete Box Beams for Highway Bridges.” *PCI JOURNAL*.

Jo, B Yung-Wan, Tea,Ghi-Ho, Kwon, Byung-Yun, (2004)." Ductility Evaluation of Prestressed Concrete Beams with CFRP Tendons." Journal of Reinforced Plastics and Composites, vol. 23, issue 8, pp. 843-859.

“ISIS.” (2007). “Prestressing Concrete Structures with Fibre-Reinforced Polymers." ISIS Canada Educational Module No.10.

Jawaheri Zadeh, H., and Nanni, A., (2013). “Reliability Analysis of Concrete Beams Internally Reinforced with Fiber-Reinforced Polymer Bars.” (110).

Kakizawa, T., Ohno, S., and Yonezawa, T., (1993) “Flexural Behavior and Energy Absorption of Carbon FRP Reinforced Concrete Beams,” FRP Reinforcement in Concrete Structures – International Symposium SP-138, American Concrete Institute, Farmington Hills, MI, 1993, pp. 585-598.

Ravindra, M. K. , and Galambos, T. V. (1978). “Load and resistance factor design for steel.”*J. Struct. Div.* , 104 (9), 1337–1353.

Shield, CK., Galambos, TV., and Gilbrandsen, P., (2011). “On The History and Reliability of The Flexural Strength of FRP Reinforced Concrete Members In ACI-440.1R.” ACI Publication

Leung, H. Y., Balendran, R. V., Rana, T. M., and Tang, W. C., (2003). “Fiber Reinforced Polymer Materials for Prestressed Concrete Srtuctures.” *Structural Survey*, 21(2), 95–101.

Merchers, Robert E., (1999)," Structural Reliability Analysis and Prediction."

Mertol, H. C., Rizkalla, S., Scott, P., Lees, J. M., and El-Hacha, R., (2006). "Durability and Fatigue Behavior of High-Strength Concrete Beams Prestressed with CFRP Bars." *ACI Special Publication SP245-1*, Case Histories and Use of FRP for Prestressing Applications, 1-20.

Mutsuyoshi H., and Machida, A., (1993). "Behavior of Prestressed Concrete Beams Using FRP as External Cable." *ACI SP-138*, American Concrete Institute,pp. 401-418.

Noël, M., and Soudki, K., (2011). "Evaluation of FRP Posttensioned Slab Bridge Strips Using AASHTO-LRFD Bridge Design Specifications." *Journal of Bridge Engineering*, (December), 839–846.

Nowak, A. `S., Park, C.-H., and Casas, J. R., (2001). "Reliability Analysis of Prestressed Concrete Bridge Girders: Comparison of Eurocode, Spanish Norma IAP and AASHTO LRFD." *Structural Safety*, 23(4), 331–344.

Nowak, A.S., (1992). NCHRP Project 12-33: "Calibration of LRFD Bridge DesignCode." Transportation Research Board, Washington, D.C.

Nowak, A. S., (1994). "Live Load Model for Highway Bridges." 13(June), 53–66.

Nowak, A. S., (1995). "Calibration of LRFD Bridge Code." *Structural Engineering*, 121(8), 1245–1251.

Nowak, A.S., (1999). NCHRP Report 368: "Calibration of LRFD Bridge DesignCode." Transportation Research Board, National Academy Press, Washington, D.C.

Nowak, A. S., Szerszen, Maria M., (2003)."Calibration of Design Code for Buildings (ACI 318): Part 1Statistical Models for Resistance" *ACI Structural Journal.*

Okeil, A. M., Belarbi, A., and Kuchma, D. a., (2012). "Reliability Assessment of FRP-Strengthened Concrete Bridge Girders in Shear." *Journal of Composites for Construction*, 17(1), 91–100.

Okeil, A. M., El-tawil, S., Asce, M., and Shahawy, M., (2002). "Flexural Reliability of Reinforced Concrete Bridge Girders Strengthened with Carbon Fiber-Reinforced Polymer Laminates." (October), 290–299.

Park, Sang Yeol, Naaman, Antoine E., (1999)."Shear Behavior of Concrete BEams Prestressd With FRP Tendons." *PCI JOURNAL*

Roddenberry, M., Mtenge, P., and Joshi, K., (2014). "Investigation of Carbon Fiber Composite Cables (CFCC) in Prestressed Concrete Piles." *FDOT*.

Sato, Y., Ueda, T., and Kakuta, Y., (1994). “Analytical Evaluation of shear Resisting Behavior of Prestressed Concrete Beams Reinforced with FRP Rods.” Transactions of the Japan Concerete Institute.

Soudki, K. A., (1998). “FRP Reinforcement for Prestressed Concrete Structures.” *Construction Research Communications Limited*.

Stoll, Frederick, Saliba, Joseph E , Casper, Laura E., (2000)," Experimental Study of CFRP-Prestressed High-Strength Concrete Bridge Beams." *Journal of Composite Structures* 49 (2000) 191–200.

TXDOT Standard Specification and Drawing (2014)

Whitehead, P. A., and Ibell, T. J., (2005). “Rational Approach to Shear Design in Fiber-Reinforced Polymer-Prestressed Concrete Structures.” *Journal of Composites for Construction*, 9, 90–100.

Wilcox, P. C., (2008). “Reliability Based Assessment of FRP Rehabilitation of Reinforced Concrete Girders.” *UC San Diego Eloctronic Theses and Dissertaions*.

URL. www.Blackburnnews.com

Umoh, Akaninyene A., Olusola, K. O., (2012). "Compressive Strength and Static Modulus of Elasticity of Periwinkle Shell Ash Blended Cement Concrete." *International Journal of Sustainable Construction Engineering & Technology* (ISSN: 2180-3242)

Yonekura, A., Tazawa, E., Zhou, P., and Sumi, H., (1994). “Mechanical Behavior of Prestrssed Concrete Beams with FRP Rods Subjected to combined Bending and Torsional Moments.”

APPENDEX A

A.1 Definitions

The bias of a random variable x is defined as the ratio of mean value of parameter μ_x to the nominal value x_n

$$\lambda_x = \frac{\mu_x}{x_n}, \qquad \textbf{Eq. A-1}$$

which is used in the design process.

The coefficient of variation of the parameter x, COV(x) is the normalized measure of dispersion of the data points. COV (x) is evaluated as the ratio of standard deviation of random variable σ_x to its mean value as

$$COV(x) = \frac{\sigma_x}{\mu_x}. \qquad \textbf{Eq. A-2}$$

Distribution type or probability distribution function is the best fit to a data set, representing the frequency of the data points. Specifically,

$$P(a < X < b) = \int_a^b f_x(x)dx, \qquad \textbf{Eq. A-3}$$

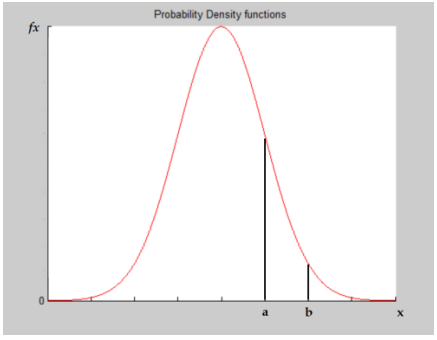

Figure A-1 Probability Distribution Function

where fx(x) is probability distribution function, a and b are the limits for variables. The total area under the probability distribution function is equal to 1 which means that it

is 100% probable to have a random number between -∞ and +∞. The probability of x being between -∞ and x is known as cumulative distribution function (CDF) which can be represented as

$$P(-\infty < X < a) = \int_{-\infty}^{a} f_x(a)dx = F_x(a). \qquad \textbf{Eq. A-4}$$

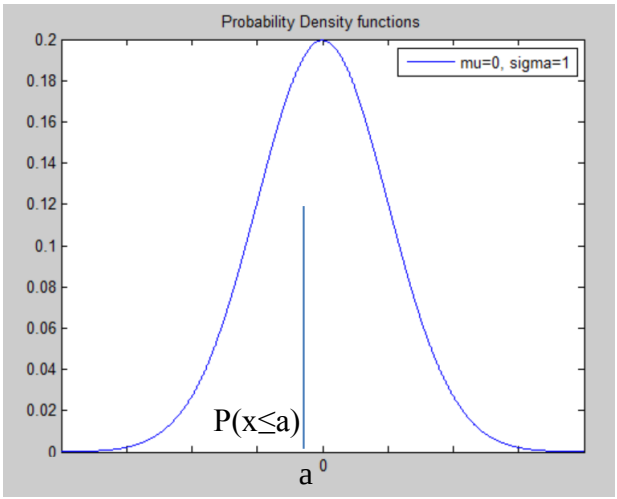

(a)

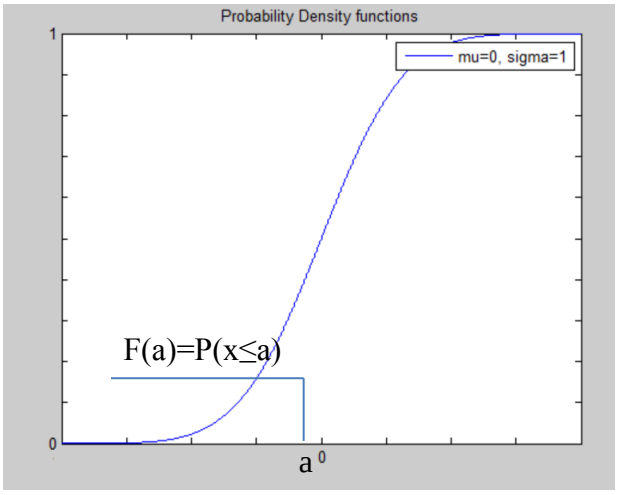

(b)

Figure A-2 Probability Distribution Function (a), Cumulative Distribution Function (b)

A statistical analysis should be performed to determine the closeness of a distribution to the dataset. The absence or presence of symmetry with respect to mean value is one of

the effective parameters in selecting the distribution type. In this study, the random variables distribution functions were taken from the literature.

The correlation coefficient is an index between -1 and 1, which measures the statistical dependency of two random variables. The correlation coefficient equal to 1 represents full linear correlation. In this case, for each generated random number for one of the variables, the second variable becomes a deterministic number. Additionally, the correlation coefficient equals to 0 refers to the cases with no dependency (correlation).

A.2 Assigned PDF

A probability distribution function was assigned to the random variables in this study. Normal or Gaussian distribution were used for all of the random variables, through an extensive literature review. Normal probability distribution function is specified by two parameters: Mean value μ, and standard deviation σ. Mean value in normal distribution corresponds to the median and mode values as well. Standard deviation illustrates the shape of the bell curve in the distribution. Increasing the dispersion, leads to decreasing the frequency of the mean value. The normal probability distribution function is captured by

$$f_x(x, \mu, \sigma) = \frac{1}{\sigma_x\sqrt{2\pi}} \exp[-\frac{1}{2}\left(\frac{x-\mu_x}{\sigma_x}\right)^2]. \quad \textbf{Eq. A-5}$$

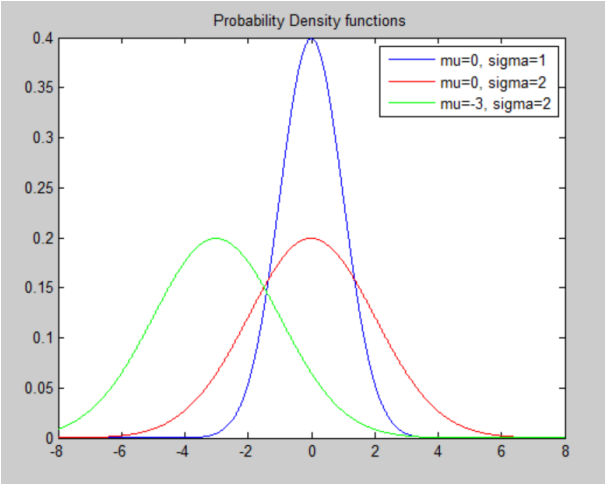

Figure A-3 Effect of Mean and Standard Deviation on Shape of Normal PDF

The CDF a normal distribution cannot be evaluated by a closed form solution. Usually, a table is used to evaluate the CDF of a normal distribution by changing the distribution to a standard normal.